

A novel chemical inhibitor of polar auxin transport promotes shoot regeneration by local enhancement of HD-ZIP III transcription

Saiqi Yang¹ , Marjolein de Haan¹, Julius Mayer¹, Dorina P. Janacek², Ulrich Z. Hammes² ,
Brigitte Poppenberger³  and Tobias Sieberer¹ 

¹Research Unit Plant Growth Regulation, TUM School of Life Sciences, Technical University of Munich, 85354 Freising, Germany; ²Plant Systems Biology, TUM School of Life Sciences, Technical University of Munich, 85354 Freising, Germany; ³Biotechnology of Horticultural Crops, TUM School of Life Sciences, Technical University of Munich, 85354 Freising, Germany

Author for correspondence:
Tobias Sieberer
Email: tobias.sieberer@tum.de

Received: 18 November 2021
Accepted: 21 April 2022

New Phytologist (2022) 235: 1111–1128
doi: 10.1111/nph.18196

Key words: auxin, chemical genetics, cytokinin, HD-ZIP III, *Helianthus annuus*, pluripotency, polar auxin transport, shoot regeneration.

Summary

- *De novo* shoot organogenesis is a prerequisite for numerous applications in plant research and breeding but is often a limiting factor, for example, in genome editing approaches. Class III homeodomain-leucine zipper (HD-ZIP III) transcription factors have been characterized as crucial regulators of shoot specification, however up-stream components controlling their activity during shoot regeneration are only partially identified.
- In a chemical genetic screen, we isolated ZIC2, a novel activator of HD-ZIP III activity. Using molecular, physiological and hormone transport analyses in *Arabidopsis* and sunflower (*Helianthus annuus*), we examined the molecular mechanism by which the drug promotes HD-ZIP III expression.
- ZIC2-dependent upregulation of HD-ZIP III transcription promotes shoot regeneration in *Arabidopsis* and is accompanied by the induction of shoot specifying factors WUS and RAP2.6L and a subset of cytokinin biosynthesis enzymes. ZIC2's effect on HD-ZIP III expression and regeneration is based on its ability to limit polar auxin transport. We further provide evidence that chemical modulation of auxin efflux can enhance *de novo* shoot formation in the regeneration recalcitrant species sunflower.
- Activation of HD-ZIP III transcription during shoot regeneration depends on the local distribution of auxin and chemical modulation of auxin transport can be used to overcome poor shoot organogenesis in tissue culture.

Introduction

Plants show a remarkable ability to regenerate in response to loss or damage of body parts. When organ forming apical meristems are lost, they can be reestablished in a process called *de novo* organogenesis (Ikeuchi *et al.*, 2019). *De novo* organogenesis is critical for plants as sessile organisms to survive adverse environmental conditions. Moreover, this process is exploited for the breeding and clonal propagation of crops and also represents a crucial prerequisite for plant biotechnological approaches such as genome editing. However, the limited or variable regeneration competence of plant tissues *in vitro* is still a main bottleneck in the application of these methodologies (Altpeter *et al.*, 2016).

De novo organogenesis is a hormone-controlled process and consists of different phases. A well-established standard system employs a two-step protocol in which first a pluripotent cell mass, called callus, is formed (Ikeuchi *et al.*, 2013). The callus induction medium (CIM) is rich in the plant hormone auxin and triggers the proliferation of cells with an identity reminiscent of

lateral root primordia. Subsequent transfer on cytokinin-rich shoot induction medium (SIM) results in the conversion of callus cells into functional shoot meristems. This is mediated by a complex patterning process, where areas of different hormone responses are established and a functional stem cell niche is formed. In recent years the temporal and spatial sequences have been described and several factors involved in this self-organizing process have been identified (Radhakrishnan *et al.*, 2018; Ikeuchi *et al.*, 2019), however a full mechanistic understanding is currently lacking and the cause for the strong genotypic variation in the regenerative responsiveness is not resolved.

A key regulatory step in *Arabidopsis* shoot regeneration is the local induction of the homeodomain transcription factor WUSCHEL (WUS), whose expression domain defines the organizing center (OC) of the shoot stem cell niche (Mayer *et al.*, 1998; Sugimoto *et al.*, 2019). Cytokinin in the SIM activates B-type ARABIDOPSIS RESPONSE REGULATORS (ARRs), who induce WUS expression by direct binding to its promoter (Meng *et al.*, 2017; T. Q. Zhang *et al.*, 2017). The locally

restricted expression of WUS is mediated by the class III homeodomain-leucine zipper (HD-ZIP III) family of transcription factors, which physically interact with B-type ARRs at the WUS promoter (T. Q. Zhang *et al.*, 2017). Next to WUS, HD-ZIP III proteins also affect the expression of other shoot identity-conferring transcription factors including SHOOT MERISTEMLESS and RAP2.6L (Shi *et al.*, 2016; Yang *et al.*, 2018). Thus, spatially restricted activation of HD-ZIP III activity is an important prerequisite of shoot regeneration, but the molecular basis of this activation is not fully understood.

Class III homeodomain-leucine zipper proteins are not only crucial for *de novo* shoot regeneration but also represent key determinants of shoot identity during embryogenesis (Prigge *et al.*, 2005; Grigg *et al.*, 2009; Smith & Long, 2010). The expression domains of HD-ZIP III family members are confined to the apical central domain of the developing embryo by the activity of the mir165/166 family of micro-RNAs (miRNAs) (Smith & Long, 2010; Miyashima *et al.*, 2013). This spatial expression pattern is further enforced by the function of AGO10, which dampens the effect of miRNA165/166 in the area of the future shoot meristem (Liu *et al.*, 2009; Zhu *et al.*, 2011). An additional level of regulation is executed by the LITTLE ZIPPER (ZPR) family of microProteins who represent direct transcriptional targets of HD-ZIP III proteins and in turn repress their activity by physical interaction (Wenkel *et al.*, 2007; Kim *et al.*, 2008).

Notably, HD-ZIP III proteins also possess two distinct putative small molecule ligand domains, implicating the presence of further yet unknown modes of regulation (Magnani & Barton, 2011). The steroidogenic acute regulatory protein-related lipid transfer (START) domain was first characterized in animal proteins where they bind diverse hydrophobic compounds (Schrack *et al.*, 2014). The C-terminal MEKHLA domain belongs to the superfamily of Per-ARNT-Sim-like (PAS-like) domains (Mukherjee & Burglin, 2006). Per-ARNT-Sim domains can act as sensors of diverse stimuli and regulate the activity of effector domains present in the same protein (Moglich *et al.*, 2009). The HD-ZIP III-specific ligands for these domains are not known to date but it was speculated that the binding status modulates their transcriptional activity as well as their dimerization behavior (Magnani & Barton, 2011; Schrack *et al.*, 2014).

In an attempt to identify novel mechanisms of HD-ZIP III regulation, we performed a reporter based small molecule screen for compounds, which increase the activity of HD-ZIP III *in planta*. We identified a novel plant growth regulator that promotes HD-ZIP III function by stimulating their transcriptional expression. Application of the compound during tissue culture enhances the shoot regeneration response of *Arabidopsis* in an HD-ZIP III-dependent manner. We further provide evidence that the regenerative function of the compound is based on its ability to limit polar auxin transport. Finally, we show that chemical modulation of auxin transport can significantly enhance shoot regeneration in sunflower (*Helianthus annuus* L.), an important oil crop, in which genetic transformation and genome editing is currently difficult to achieve due to its poor shoot formation capacity in tissue culture (Zhang & Finer, 2015).

Materials and Methods

Plant materials and growth conditions

Unless stated otherwise, *Arabidopsis thaliana* (L.) Heynh. seeds were plated and plants grown as described in the literature (Yang *et al.*, 2018). Previously published plant lines used in this study: *phb-1d* (McConnell *et al.*, 2001), *rev-10d*, *rev-6 phb-13 phv-11* (Prigge *et al.*, 2005), *pZPR::ZPR3::β-glucuronidase (GUS)* and *35S::ZPR3* (Wenkel *et al.*, 2007), *pWUS::GUS* (Gross-Hardt *et al.*, 2002), *pRAP2.6L::RAP2.6L::GUS* (Yang *et al.*, 2018), *pPHB>>GFP*, *pMIR165A::GFP* and *pMIR166A::GFP* (Carlsbecker *et al.*, 2010), *gPHB::GUS* (Gillmor *et al.*, 2010), *pIPT1::GUS* and *pIPT5::GUS* (Miyawaki *et al.*, 2004), *pIPT7::GFP* (Takei *et al.*, 2004), *pARR5::GUS* (D'Agostino *et al.*, 2000), *TCS::GFP* (Muller & Sheen, 2008), *DR5::GUS* (Ulmasov *et al.*, 1997), *DR5rev::GFP* and *pPIN1::GUS* (Friml *et al.*, 2003), *pPIN1::PIN1::GFP* (Benkova *et al.*, 2003).

Chemical screen

Compounds of a custom assembled chemical library (www.chembridge.com) were tested in half-strength Murashige & Skoog (MS) liquid medium under the growth conditions described earlier at a final concentration of 25 μM. The *pZPR3::GUS* seeds were germinated in the presence of the compounds until day 10. Seedlings were subjected to GUS staining and analyzed with a stereomicroscope (SZX10; Olympus, Tokyo, Japan). ZIC2 (Chembridge ID: 5131153) and the described structural analogs were re-ordered from MolPort (www.molport.com) with the following ID numbers: ZIC2 (000-246-311), T1 (000-759-143), T2 (002-287-475), T3 (000-251-109), T4 (001-534-280), T5 (002-251-423), T6 (009-332-327), T7 (000-205-112), L1 (009-030-711), L2 (000-650-194), P1 (000-246-278), P2 (009-146-001), P3 (001-679-944), P4 (009-509-050), P5 (000-780-505).

Gene constructs

Polymerase chain reaction (PCR) was performed with proofreading thermostable polymerase (Thermo Fisher Scientific, Waltham, MA, USA), and all clones were confirmed by sequencing. For generation of *pZPR3::GUS*, the 3132 bp promoter region of *ZPR3* gene (AT3G52770) was amplified with primers pZPR3F(PstI) and pZPR3R-2(BamHI) and subcloned into pGEM-T Easy (Promega, Madison, WI, USA). The fragment was excised using PstI and BamHI and ligated into pPZP-GUS-1 (Diener *et al.*, 2000). At least 10 independent *pZPR3::GUS* transgenic lines were generated, which showed the same tissue-specific expression pattern. For generation of *pZPR3::LUC* the 3132 bp upstream promoter region of *ZPR3* gene (AT3G52770) was amplified with primers pZPR3F(PstI) and pZPR3R-2(NcoI) and inserted as PstI/NcoI fragments into corresponding cloning sites of the transient expression vector pGreenII 0800-LUC (Hellens *et al.*, 2000). To create effector vectors 35S::PHB-YFP and 35S::REV-YFP, the open reading frame (ORF) of PHABULOSA (AT2G34710) and REVOLUTA (AT5G60690) were amplified

by PCR using PHB ORF F (EcoRV)-PHB ORF R (NotI) and REV ORF F (EcoRV) and REV ORF R (NotI), respectively. The fragments were subcloned into pGEM-T Easy. Subsequently, the PHB ORF and REV ORF were transferred via EcoRV and NotI into pGWR8-YFP (Rozhon *et al.*, 2010), and NotI excised the yellow fluorescent protein (YFP) sequence of pGWR8-YFP out. YFP (from pGWR8-YFP) was subcloned into NotI site of pGWR8-PHB and pGWR8-REV.

GUS staining

GUS staining was performed as previously described (Yang *et al.*, 2018). The seedlings were stained at 37°C for various periods of time depending on the reporter strength. After staining the tissue was dehydrated with 70% ethanol. Samples were analyzed using a stereomicroscope (SZX10; Olympus).

Fluorometric MUG assay

The *pZPR3::GUS* seedlings were grown on half-strength MS medium (½MS) under the growth conditions described earlier containing 25 µM of ZIC2 or the described structural analogs. The roots were harvested and flash-frozen in liquid nitrogen. The MUG assay was performed as previously described (He *et al.*, 2018).

Fluorescence microscopy

Images of *pPHB>>GFP*, *TCS::GFP*, *pIPT7::GFP*, *pPIN1::PIN1::GFP* and *DR5rev::GFP* tissues were generated using a TCS SP8 (Leica Microsystems, Wetzlar, Germany) or a FV1000 (Olympus) confocal laser-scanning microscope. Green fluorescent protein (GFP) was excited at 488 nm and emission was analyzed between 500–535 nm.

Protoplast transactivation assay

Protoplasts were isolated and transformed as described in Yoo *et al.* (2007). Thus, 14 h after transformation, protoplasts were harvested by centrifuging at 100 g for 2 min at room temperature and flash-frozen in liquid nitrogen. Luciferase assays were performed using a Dual-Luciferase Reporter Assay System (Promega) with a Lumat LB9501 luminometer (Berthold, Bad Wildbach, Germany) for signal quantification.

Lugol staining

Roots of 7-d-old seedlings were stained with Lugol's solution (Sigma-Aldrich) for 3 min, then transferred to clearing solution (chloral hydrate:water:glycerol, 8:3:1, v/v) and imaged immediately with a stereomicroscope (SZX10; Olympus).

Auxin transport assay

Auxin transport measurement was performed based on a previous protocol with minor modifications (Xiao & Offringa, 2020).

Four 2.5-cm segments from the basal part of 15-cm long wild-type (WT) Col-0 inflorescence stems were placed in inverted orientation in 30 µl of auxin transport buffer (0.5 nM indole-3-acetic acid (IAA), 1% sucrose, 5 mM MES, pH 5.5) with either solvent control, 50 µM naphthylphthalamic acid (NPA) or 50 µM ZIC2 for 1 h, then transferred to 30 µl of auxin transport buffer with either solvent control, 50 µM NPA or 50 µM ZIC2 containing 2 µM [¹⁴C] IAA (Biotrend, Köln, Germany), allowed to incubate for 1 h and subsequently transferred to 30 µl of auxin transport buffer without [¹⁴C] IAA and incubated for another 4 h. Segments were cut into 5-mm pieces, the bottom piece (0–5 mm) was discarded and the remaining pieces were placed separately into 2 ml of Ultima-Flo AF (no. 6013589; PerkinElmer, Waltham, MA, USA) for overnight maceration. [¹⁴C] IAA was quantified using a Tri-Carb 2800TR liquid scintillation analyzer (PerkinElmer).

PIN transport assay

The transport assays for PIN1 and PIN3 in oocytes were performed as previously described (Fastner *et al.*, 2017). ZIC2 (10 µM final internal concentration) was coinjected with ³H-IAA (RC Tritec, Teufen, Switzerland).

Arabidopsis shoot regeneration assay

The assay was performed based on a previous protocol with minor modifications (Che *et al.*, 2006). *Arabidopsis* seeds were germinated and grown for 8 d on ½MS under long day conditions. Root segments of 1.5–2 cm were cut, transferred to CIM (full strength MS medium including B5 vitamins (Duchefa, Haarlem, the Netherlands) supplemented with 0.5 g l⁻¹ MES (pH set to 5.7), 2% sucrose, 2.2 µM 2,4-dichlorophenoxyacetic acid, 0.2 µM kinetin and 0.8% agar) and incubated under constant light (80 µmol s⁻¹ m⁻², 21°C) for 4 d. The root explants were then transferred to shoot induction medium (full strength MS medium including B5 vitamins (Duchefa) supplemented with 0.5 g l⁻¹ MES (pH set to 5.7), 2% sucrose, 2.5 µM isopentenyladenine, 0.45 µM IAA and 0.8% agar) and incubated under constant light (80 µmol s⁻¹ m⁻², 21°C) for 16 d.

Sunflower shoot regeneration assay

The sunflower regeneration protocol was modified based on previous protocols (Sujatha *et al.*, 2012; Radonic *et al.*, 2015). Seeds from the *Helianthus annuus* L. inbred line HA89 were rinsed with 70% ethanol, soaked in 5% sodium hypochlorite (NaOCl) containing 0.05% Tween 20 for 15 min with mild shaking, followed by three washes with sterile double-distilled water (ddH₂O). The seeds were de-coated after 30 min soaking in sterile ddH₂O, re-sterilized and germinated overnight on ½MS in the dark at 26°C. Then the seed radicles were cut off and the internal thin membrane was removed. The rest of the seed was separated longitudinally along the embryo axis, and the leaf primordia at the base of the cotyledons were removed. The cotyledons were placed on coculture medium (MS

medium with B5 vitamins (Duchefa; pH set to 5.8) with 3% sucrose and 3 g l⁻¹ phytigel, supplemented with 2.0 mg l⁻¹ isopentenyladenine, 0.5 mg l⁻¹ IAA and 0.1 mg l⁻¹ thidiazuron) with the adaxial side in contact with the medium. The cotyledon explants were cultured at 30 μmol m⁻² s⁻¹ light intensity, at 24°C (±2°C) under long day conditions (16 h : 8 h) for 10 d, then subcultured on coculture medium for another 11 d. The shoot apical meristem (SAM) cluster area was measured with IMAGEJ software. For shoot elongation, explants were transferred to coculture medium supplemented with 0.1 mg l⁻¹ gibberellic acid (GA₃) for 2 wk.

Quantitative real-time PCR

Approximately 50 mg of *Arabidopsis* seedling material or 200 mg of sunflower cotyledon explants were collected, shock-frozen in liquid nitrogen and homogenized with a Retsch mill (Verder Scientific, Haan, Germany). RNA extraction, complementary DNA (cDNA) synthesis and quantitative polymerase chain reaction (qPCR) were done as described in Yang *et al.* (2018). Sequences of oligos used for qPCR can be found in Supporting Information Table S1. Data were normalized to *AtUBC* (*AT5G25760*) or *HaACT7* (*LOC110909803*) and measured in at least three technical replicates.

Scanning electron microscopy

Sunflower seed explants were incubated in FAA fixative (50% ethanol, 10% acetic acid, 5% formaldehyde) overnight at 4°C, dehydrated through a graded ethanol series and subsequently subjected to supercritical point drying using an EM CPD300 (Leica, Wetzlar, Germany). Explants were mounted on conductive adhesive tabs (Plano, Wetzlar, Germany). Pictures were taken with a T-3000 scanning electron microscope (Hitachi, Tokyo, Japan).

Histology

The histological analysis was performed as previously described (De Smet *et al.*, 2004). Tissues were fixed overnight at 4°C in FAA (5% (v/v) formaldehyde, 5% (v/v) acetic acid, and 50% (v/v) ethanol). Samples were then dehydrated in a graded ethanol series and embedded with Technovit 7100 (Heraeus Kulzer, Hanau, Germany) according to the manufacturer's instructions. A series of 5–7 μm thick transverse sections was made with a Leica RM2255 Microtome. Sections were transferred to microscopic slides (Marienfeld, Lauda-Königshofen, Germany), stained in Ruthenium red solution (0.05%) for 50 s and rinsed with water. Stained sections were analyzed with a microscope (BX-61; Olympus).

Statistics

All statistical parameters of the performed experiments are shown in the figures or figure legends, including number of samples (*n*), type of statistical tests and methods used. Statistical significance is denoted by lower case letters, stars or the shown *P*-values.

Statistical analysis was performed with PRISM8 software (GraphPad, San Diego, CA, USA).

Results

Identification of ZIC2 in a screen for compounds that activate the expression of the HD-ZIP III direct target gene ZPR3

There is circumstantial evidence that HD-ZIP III activity is regulated by unknown signaling molecules, through interaction with the putative ligand binding domains found in these proteins (Magnani & Barton, 2011; Schrick *et al.*, 2014). We reasoned that a small molecule screen for activators of HD-ZIP III function might not only provide information about the structural requirements to interact with these domains but also might lead to the identification of novel chemical tools, to improve shoot regeneration in recalcitrant crop plants.

To this end we screened a library of 9000 structurally diverse chemicals for compounds, which induce the activity of a transcriptional GUS reporter for the HD-ZIP III direct target gene *ZPR3* (Fig. 1a). Application of 3-chloro-*N*-(1,5-dimethyl-3-oxo-2-phenyl-2,3-dihydro-1H-pyrazol-4-yl)-1-benzothiophene-2-carboxamide (CAS-RN: 301157-28-8) at a concentration of 25 μM (Fig. 1b), drastically increased pZPR3::GUS activity in seedling roots (Fig. 1c) and we therefore named the substance ZPR3 Inducing Compound 2 (ZIC2). ZIC2 also enhanced the expression of the translational reporter pZPR3::ZPR3:GUS, in the root and the shoot meristem region (Fig. 1d) and significantly increased endogenous *ZPR3* transcript levels in WT seedlings treated for 24 h with the chemical (Fig. 1e).

Next, we assessed the concentration range in which ZIC2 affects *ZPR3* expression (Fig. S1a). Root meristem specific activity of pZPR3::GUS was visibly increased at a concentration of 1 μM ZIC2 and gradually became more intense at higher concentrations. We also analyzed the kinetics of ZIC2-mediated pZPR3::GUS induction in liquid medium (Fig. S1b). A slight increase of *ZPR3* expression in the central root meristem was already visible after 1 h of ZIC2 exposure and after 3–6 h the pZPR3::GUS activity was clearly elevated in the central root meristem and the root differentiation zone. In the shoot tissues the *ZPR3* reporter activity was upregulated after 24 h under these conditions (Fig. S1b).

To specify the cell types affected by ZIC2-mediated *ZPR3* induction we analyzed reporter activity in transversal sections of root meristems. In untreated controls pZPR3::GUS activity was faintly detectable in the xylem and the adjacent procambial cells (Fig. 1f) substantially overlapping with the expression domains of HD-ZIP III transcription factors (Carlsbecker *et al.*, 2010). The reporter activity strongly increased in these tissues after 24 h of ZIC2 treatment and even expanded to the phloem and pericycle cells (Fig. 1f). Long-term ZIC2 treatment provoked a strong proliferation of stele cells in the distal root meristem, which showed intense reporter expression (Fig. 1g). Taken together, ZIC2 rapidly induces *ZPR3* transcription in a dose-dependent manner in tissues of HD-ZIP III expression.

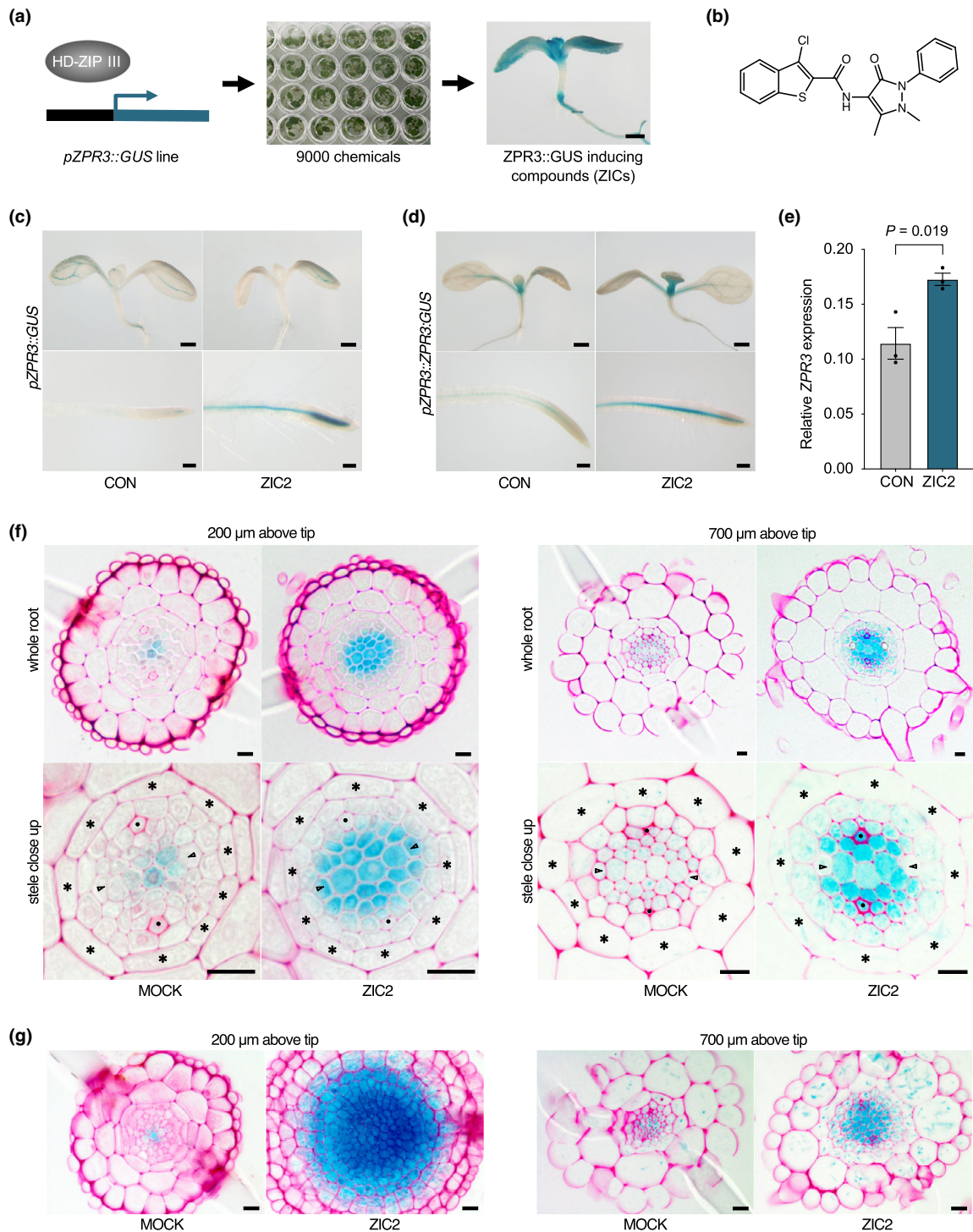


Fig. 1 Identification of ZIC2 in a screen for compounds inducing expression of the class III homeodomain-leucine zipper direct target gene ZPR3 in *Arabidopsis*. (a) Schematic representation of the screening procedure. pZPR3::GUS seedlings were germinated in liquid medium containing 9000 structurally diverse compounds at a concentration of 25 μM and subsequently ZPR3::GUS activity was subsequently determined 7 d after germination (DAG). (b) Molecule structure of ZIC2 (3-chloro-N-(1,5-dimethyl-3-oxo-2-phenyl-2,3-dihydro-1H-pyrazol-4-yl)-1-benzothiothiophene-2-carboxamide). (c) pZPR3::GUS activity in seedlings at 7 DAG, grown on solid medium containing solvent only (CON) or 25 μM ZIC2. (d) pZPR3::ZPR3::GUS activity in seedlings grown for 8 d on solid 1/2MS medium and then transferred for 24 h to liquid 1/2MS medium CON or 25 μM ZIC2. (e) Quantitative polymerase chain reaction (qPCR) analysis of ZPR3 expression in seedlings grown for 9 d on solid 1/2MS medium and then transferred for 24 h to liquid 1/2MS medium CON or 25 μM ZIC2 (means ± SEM; n = 3). P-value is indicated above bars (unpaired Student's two-tailed t-test). (f) Short-term effect of ZIC2 on tissue-specific ZPR3::GUS activity in root meristems. Transversal sections at the indicated positions of GUS-stained root tips from 7-d-old pZPR3::GUS seedlings. Before harvest plants were grown for 24 h in liquid medium containing solvent only (mock) or 25 μM ZIC2. Asterisks, endodermis; arrowheads, protoxylem; closed circles, phloem centre. (g) Long-term effect of ZIC2 on tissue-specific ZPR3::GUS activity in root meristems. Transversal sections of GUS-stained root tips of 7-d-old pZPR3::GUS seedlings grown in the absence (mock) or presence (ZIC2) of 25 μM ZIC2. Bars: (a, c, d) 500 μm; (f, g) 10 μm.

Structural requirements of ZIC2 function

To define the structural requirements for ZIC2 to activate ZPR3 expression we tested 14 structural variants showing modifications either in the thiobene ring, linker region, or the pyrazole substructure of the molecule (Fig. S2a). Whereas the linker and pyrazole variants did not show obvious induction of pZPR3::GUS activity in root tips, reporter expression was increased in the presence of T1, T3, T4, T5 and T6 (Fig. S2b,c). Quantification of GUS activity using the MUG assay revealed significant induction of root specific reporter expression by T1, T3 and T6 with all

being in a similar range as ZIC2 (Fig. S2f). Since ZIC2 negatively affects primary root elongation we also quantified root lengths of seedlings grown in the presence of the ZIC2 analogs. From the thiobene variants, T1, T3 and T6 showed the strongest negative impact on root growth (Fig. S2d). The pyrazole variant P4 also significantly suppressed root elongation, however in combination with a general toxic effect on seedling growth (Fig. S2e). Taken together, modifications in the linker and pyrazole part of ZIC2 causes loss of ZPR3 induction and root growth inhibition, whereas the thiobene moiety appears to be less important for ZIC2 function.

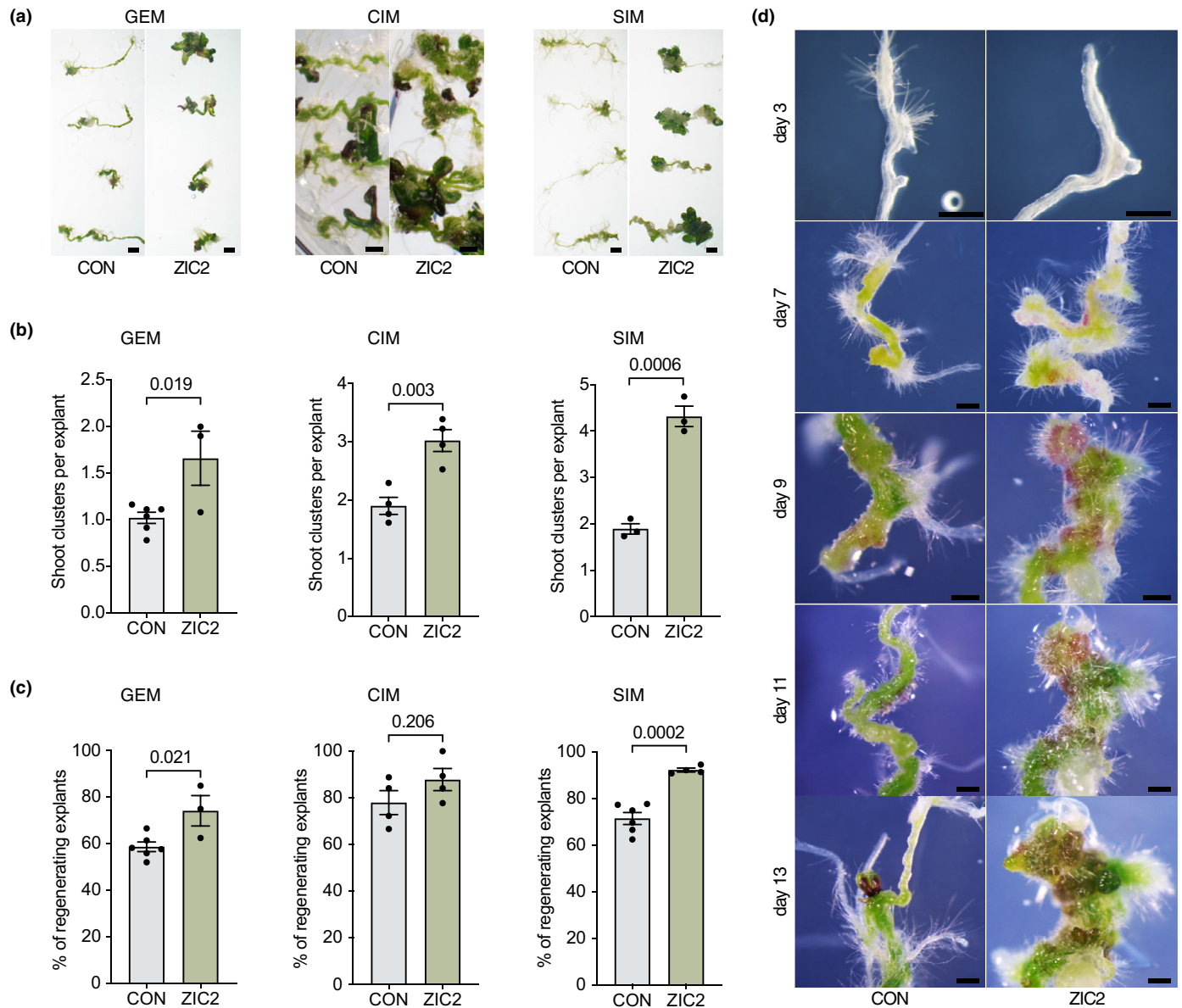


Fig. 2 ZIC2 induces shoot regeneration in *Arabidopsis*. (a) Shoot regeneration assay with root explants from wild-type (WT) seedlings where ZIC2 (25 μ M) was applied to the germination medium (GEM), the callus induction medium (CIM) or the shoot induction medium (SIM). Representative explants were photographed 13 d (GEM) or 20 d (CIM and SIM) after transfer on SIM. CON, containing solvent only. (b) Quantification of regenerated shoot clusters per explant from the regeneration assay shown in (a). Data are from at least three independent experiments (means \pm SEM). *P*-value is indicated above bars (unpaired Student's two-tailed *t*-test). (c) Quantification of percentage of explants with regenerated shoots from the regeneration assay shown in (a). Data are from at least three independent experiments (means \pm SEM). *P*-value is indicated above bars (unpaired Student's two-tailed *t*-test). (d) Phenotypes of explants cultured on SIM CON or 25 μ M ZIC2 for the indicated number of days. Bar, 500 μ m.

ZIC2 promotes shoot regeneration in *Arabidopsis*

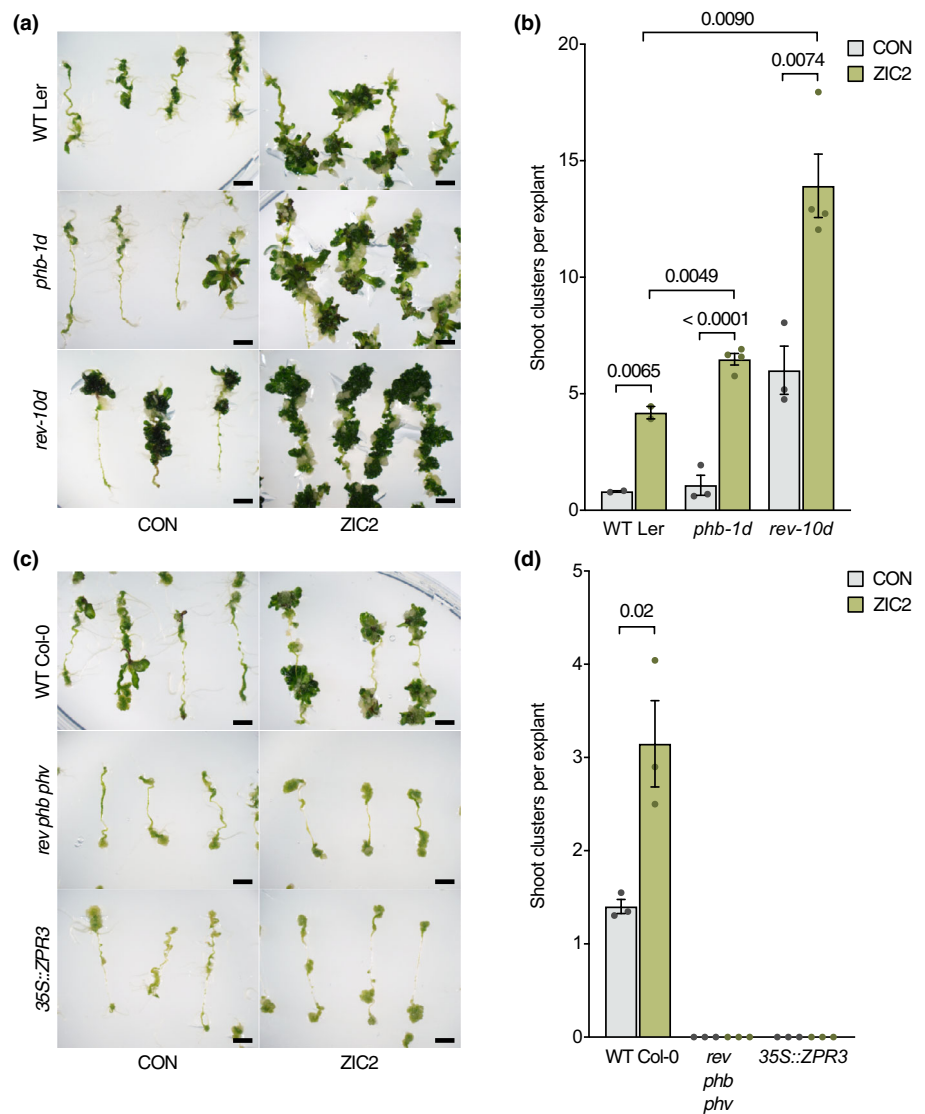
Since ZIC2 induces the transcription of the HD-ZIP III-regulated gene ZPR3 and HD-ZIP III function has been shown to be rate-limiting for shoot regeneration, we tested the effect of the chemical in a standard *Arabidopsis* regeneration assay. In this assay, seeds are germinated on 1/2MS medium, root explants are then transferred to CIM followed by an incubation on SIM. When ZIC2 was applied only during the germination phase, it negatively affected explant size (Fig. 2a), but still induced the formation of a significant higher number shoot clusters (Fig. 2a,b) and also increased the percentage of regenerating explants compared to the control (Fig. 2c). Adding ZIC2 only to the CIM enhanced the density of formed shoots per explant (Fig. 2a,b) but the number of responding explants was not significantly increased (Fig. 2c). The strongest effects were observed when ZIC2 treatment was restricted to the SIM, where two-times more shoot clusters were formed compared to the control group (Fig. 2a,b) and also the ratio of responding explants was considerably higher (Fig. 2c). Closer inspection of the explants over time

revealed that ZIC2 in the SIM suppresses the outgrowth of lateral roots and instead provokes a slightly faster and much more pronounced formation of anthocyanin rich shoot pro-meristems without having an obvious effect on the callus proliferation rate (Fig. 2d). Notably, ZIC2 did not provoke short-term induction of DR5::GUS or pARR5::GUS reporter activities indicating that the compound's effect on regeneration is not based on direct auxin or cytokinin-like activities of the molecule (Fig. S3a,b). Finally, we also tested the three thiobene analogs of ZIC2 in the shoot regeneration assay, which have shown induction of ZPR3::GUS activity. Whereas T1 and T3 rather dampened the shoot regeneration rate, T6 exerted a significant promotive effect to a similar extend as ZIC2 (Fig. S4a,b).

ZIC2 promotes shoot regeneration in a HD-ZIP III-dependent manner

Next, we asked, whether HD-ZIP III proteins are required for the promotive effect of ZIC2 on shoot regeneration. To this end

Fig. 3 The promotive effect of ZIC2 on *Arabidopsis* shoot regeneration depends on class III homeodomain-leucine zipper transcription factors. (a) Shoot regeneration phenotypes of wild-type (Ler), *phb-1d* and *rev-10d* explants cultivated on shoot induction medium (SIM) containing solvent only (CON) or 25 μ M of ZIC2. Photographs were taken 16 d after transfer on SIM. (b) Quantification of shoot regeneration rate (shoot clusters per explant) in wild-type (Ler), *phb-1d* and *rev-10d* explants cultivated on SIM CON or 25 μ M of ZIC2. Bars show means \pm SEM from at least two independent experiments ($n \geq 12$ for each experiment). *P*-value is indicated above bars (unpaired Student's two-tailed *t*-test). (c) Shoot regeneration phenotypes of wild-type (Col-0), *rev phb phv* and *35S::ZPR3* explants cultivated on SIM CON or 25 μ M of ZIC2. Photographs were taken 16 d after transfer on SIM. (d) Quantification of shoot regeneration rate (shoot clusters per explant) in wild-type (Col-0), *rev phb phv* and *35S::ZPR3* explants cultivated on SIM CON or 25 μ M of ZIC2. Bars show means \pm SEM from at least three independent experiments ($n \geq 12$ for each experiment). *P*-value is indicated above bars (unpaired Student's two-tailed *t*-test). Bar, 2 mm.



we analyzed the ZIC2-mediated regeneration response in different genotypes with altered HD-ZIP III activities. Mutation of the miRNA165/166-binding site in *phb-1d* results in ectopic accumulation of PHB (Mallory *et al.*, 2004). ZIC2-treated *phb-1d* explants showed a significantly higher shoot regeneration rate compared to the ZIC2 treated WT control whereas the untreated samples showed a similar response in our assay (Fig. 3a,b). The miRNA-resistant *rev-10d* gain-of-function allele already exerted

pronounced shoot formation under control conditions (Fig. 3a, b). However, ZIC2 treatment further enhanced the response to the brink of saturation, since there was barely any explant area left not covered with leaf primordia. To test the ZIC2 effect in plant lines with reduced HD-ZIP III function we employed the triple mutant *rev phb phv*. In accordance with a previous study (T. Q. Zhang *et al.*, 2017) *rev phb phv* explants were not able to regenerate shoots under control conditions (Fig. 3c,d). ZIC2 application

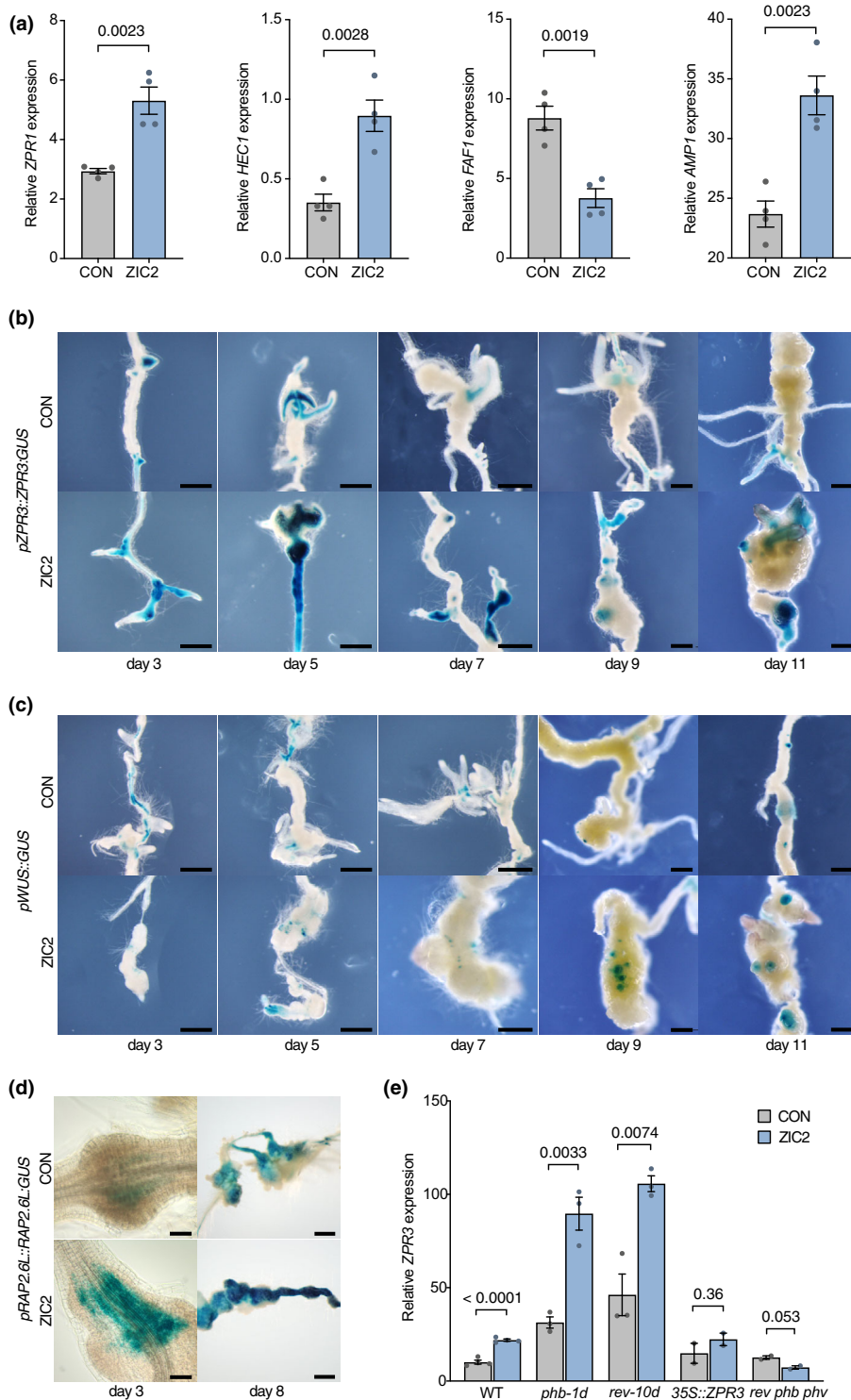


Fig. 4 ZIC2 causes advanced expression of Class III homeodomain-leucine zipper direct target genes in *Arabidopsis*. (a) Quantitative polymerase chain reaction (qPCR) expression analysis of indicated genes in roots of seedlings grown for 9 d on solid 1/2MS medium and then transferred for 24 h to liquid 1/2MS medium containing solvent only (CON) or 25 μM ZIC2. Data from four biological repeats are shown (means ± SEM). P-value is indicated above bars (unpaired Student's two-tailed t-test). (b) pZPR3::ZPR3::GUS activity in explants cultured on shoot induction medium (SIM) CON or 25 μM ZIC2 for the indicated number of days. (c) pWUS::GUS activity in explants cultured on SIM CON or 25 μM ZIC2 for the indicated number of days. (d) pRAP2.6L::RAP2.6L::GUS activity in explants cultured on SIM CON or 25 μM ZIC2 for the indicated number of days. (e) qPCR analysis of ZPR3 expression in roots of the indicated genotypes grown for 9 d on solid 1/2MS medium and then transferred for 24 h to liquid 1/2MS medium CON or 25 μM ZIC2. Data from two to four biological repeats are shown (means ± SEM). P-value is indicated above bars (unpaired Student's two-tailed t-test). Bars: (b, c and right panel in d) 500 μm; (left panel in d) 50 μm.

did not alleviate this effect. To test the ZIC2 response in a line with a minimal residual level of REV/PHB/PHV function we used *35S::ZPR3*. Again, ZIC2 was fully ineffective to promote regeneration of shoots in this genotype, supporting the conclusion that ZIC2 function is dependent on the presence of HD-ZIP III activity (Fig. 3c,d).

ZIC2 causes advanced expression of HD-ZIP III direct target genes

To assess, whether ZIC2 affects HD-ZIP III-dependent transcriptional activity on a broader level, we analyzed the expression of additional genes, directly controlled by HD-ZIP III transcription factors (Reinhart *et al.*, 2013; Weits *et al.*, 2019). A 24-h treatment with ZIC2 caused significant upregulation of ZPR1, HEC1 and AMP1 in root tissues (Fig. 4a). Long-term treatment of root explants on SIM showed ZIC2-dependent upregulation of ZPR3

expression at all tested time points (Fig. 4b). In contrast, upregulation of the HD-ZIP III target WUS (T. Q. Zhang *et al.*, 2017) became apparent only between day 7 and 9 after transfer on SIM containing ZIC2 (Fig. 4c). Finally, we also followed the expression of RAP2.6L in response to ZIC2, an AP2 transcription factor with a rate limiting effect on shoot regeneration, whose transcription is directly activated by HD-ZIP III proteins (Che *et al.*, 2006; Yang *et al.*, 2018). GUS-activity of a RAP2.6L-specific reporter was elevated in the presence of ZIC2 from day 3 onward and cumulated at day 8 under the used conditions (Fig. 4d).

To interrogate, whether the observed induction of HD-ZIP III target genes by ZIC2 is indeed dependent on HD-ZIP III activity, we compared the amplitude of ZPR3 activation in different HD-ZIP III gain and loss of function alleles by qPCR (Fig. 4e). As expected, *ZPR3* messenger RNA (mRNA) levels were elevated in *phb-1d* and *rev-10d* compared to WT. In both genotypes ZIC2 application for 24 h resulted in a further boost of ZPR3

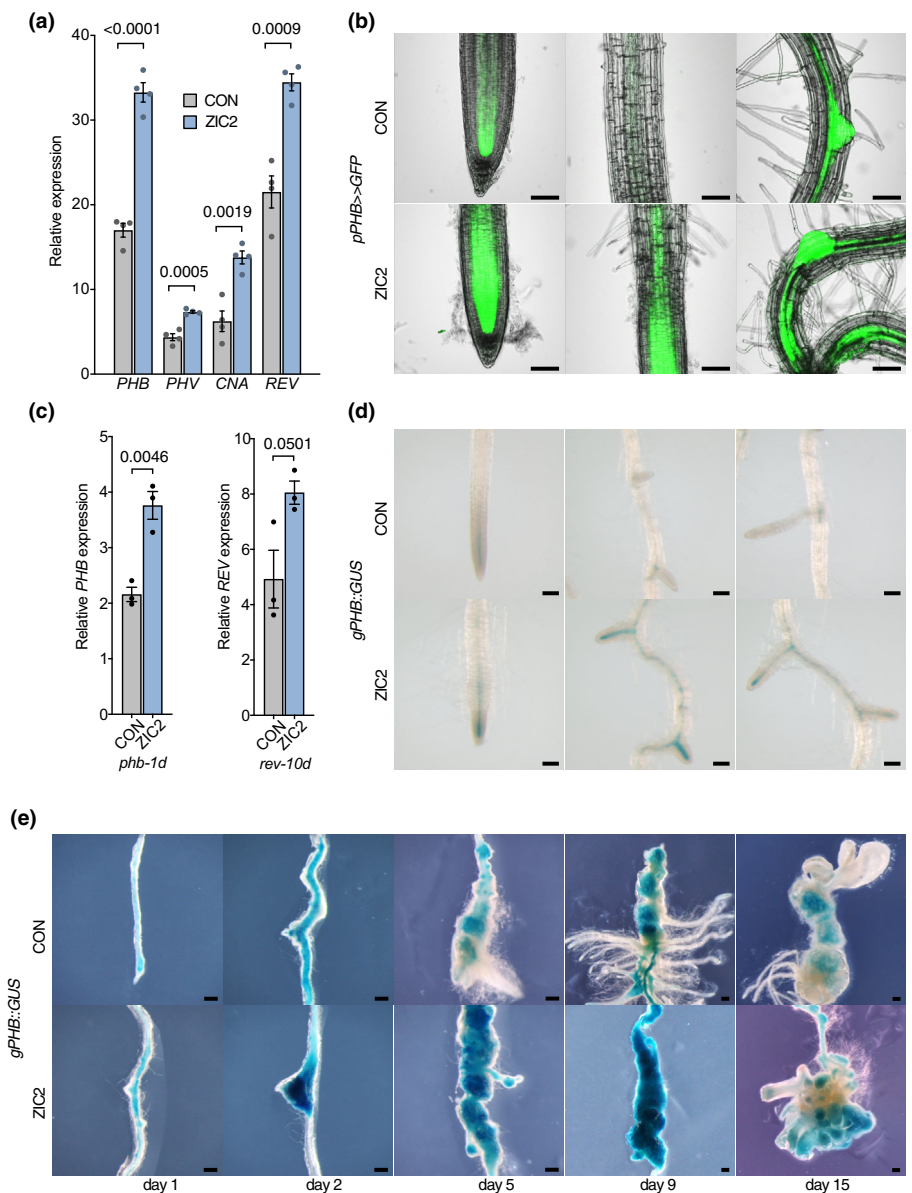


Fig. 5 ZIC2 promotes the transcription of Class III homeodomain-leucine zipper proteins. (a) Quantitative polymerase chain reaction (qPCR) expression analysis of indicated genes in roots of seedlings grown for 9 d on solid $\frac{1}{2}$ MS medium and then transferred for 24 h to liquid $\frac{1}{2}$ MS medium containing solvent only (CON) or 25 μ M ZIC2. Data from four biological repeats are shown (means \pm SEM). *P*-value is indicated above bars (unpaired Student's two-tailed *t*-test). (b) pPHB::GFP fluorescence in roots of seedlings grown for 5 d on solid $\frac{1}{2}$ MS medium and then transferred for 48 h to liquid $\frac{1}{2}$ MS medium CON or 25 μ M ZIC2. (c) qPCR expression analysis of indicated genes in roots of *phb-1d* (left graph) and *rev-10d* (right graph) seedlings grown for 9 d on solid $\frac{1}{2}$ MS medium and then transferred for 24 h to liquid $\frac{1}{2}$ MS medium CON or 25 μ M ZIC2. Data from three biological repeats are shown (means \pm SEM). *P*-value is indicated above bars (unpaired Student's two-tailed *t*-test). (d) gPHB::GUS activity in roots of seedlings grown for 7 d on solid $\frac{1}{2}$ MS medium and then transferred for 24 h to liquid $\frac{1}{2}$ MS medium CON or 25 μ M ZIC2. (e) gPHB::GUS activity in explants cultured on shoot induction medium (SIM) CON or 25 μ M ZIC2 for the indicated number of days. Bars: (b) 50 μ m; (d) 100 μ m; (e) 200 μ m.

transcript levels (Fig. 4e). In contrast, ZIC2 induction of ZPR3 transcripts (qPCR specific for non-transgenic mRNAs) was diminished in *35S::ZPR3* and absent in *rev phb phv* (Fig. 4e).

ZIC2 induces HD-ZIP III transcription

To test whether ZIC2 affects HD-ZIP III function at the protein level, e.g. by interacting with one of the ligand binding domains, we overexpressed PHB and REV in protoplasts and compared the induction rates of the ZPR3 promoter in the presence of increasing concentrations of ZIC2 (Fig. S5). Neither PHB nor REV-dependent activation of the pZPR3::LUC reporter changed in the presence of ZIC2 indicating that the compound does not primarily affect HD-ZIP III protein function.

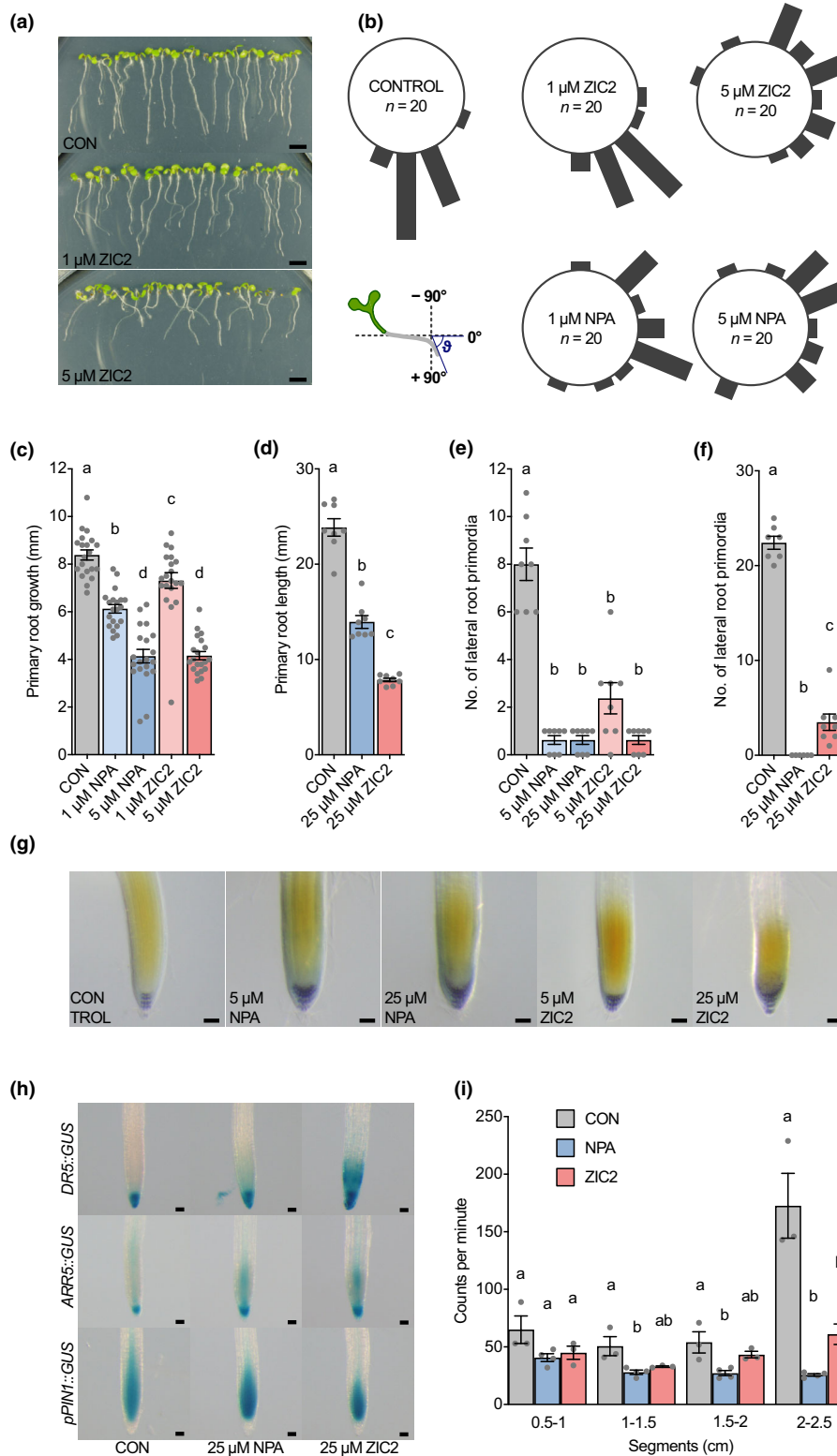
A 24 h ZIC2 treatment of seedlings rather caused a significant increase of transcript levels of all four tested members of the HD-ZIP III family (Fig. 5a). Analysis of the pPHB>>GFP reporter in ZIC2-treated roots revealed a stronger fluorescence in the original expression domain, as well as a lateral expansion in the root meristem (Fig. 5b). Increased reporter activity was also visible in the stele along the root axis (Fig. 5b). The ZIC2-mediated induction of transcription was also detectable in the miRNA-resistant HD-ZIP III mutants *phb-1d* and *rev-10d* (Fig. 5c), indicating that ZIC2 acts in a miRNA165/166-independent manner. Consistent with this assumption, 24 h ZIC2 treatment did not drastically change the expression patterns of pMIR165A::GFP and pMIR166A::GFP in the root meristem endodermis (Fig. S6a,b). After 48 h the reporter activities became more restricted to the proliferation zone, which appeared to be a consequence of the morphological change of the meristem. Enhanced *PHB* transcription levels by ZIC2 application in roots correlated with higher PHB protein accumulation as denoted by the stronger GUS activity of the gPHB::GUS reporter (Fig. 5d). We also monitored gPHB::GUS activity in root explants shifted on SIM containing ZIC2

(Fig. 5e). From day 2 onward, strong reporter activation could be observed in proliferating areas in ZIC2-treated explants, which were localized in bigger but also more irregular foci compared to the mock control. Reporter expression further intensified in ZIC2-treated explants from day 5 to day 9 causing strong GUS staining of the entire propagule, whereas reporter activity in the control was restricted to separated patches.

ZIC2 induces the expression of a subset of cytokinin biosynthesis enzymes during shoot regeneration

PHB has been shown to promote the expression of a subset *IPT* genes in the root apical meristem, which code for rate limiting enzymes of cytokinin biosynthesis (Dello Ioio *et al.*, 2012). ZIC2 treatment significantly elevated the transcript levels of *IPT1*, *IPT3* and *IPT7* in roots (Fig. S7a). Consistent with the qPCR data, pIPT1::GUS and pIPT7::GFP activity was increased in the basal stele, 24 h after addition of ZIC2, and the expression domains of the reporters expanded to the whole root meristem area after prolonged ZIC2 treatment (Fig. S7b,c). The elevated expression of *IPT* genes correlated with a higher activity of the cytokinin-responsive reporter pARR5::GUS in root meristematic tissues (Fig. S7d). Next, we monitored IPT reporter expression in root explants during the shoot regeneration process. A ZIC2-dependent increase of pIPT1::GUS activity was first apparent 5 d after transfer on SIM and further intensified at day 7 to day 10 (Fig. S7e). IPT7::GFP fluorescence was also clearly elevated in the outer layers of explants grown on ZIC2-containing SIM (Fig. S7f). Using TCS::GFP and pARR::GUS, we could detect a ZIC2-mediated stronger cytokinin response in explant tissue domains showing the pronounced IPT1 and IPT7 expression levels (Fig. S7g,h). Notably, the expression of IPT5, a gene which has been reported to be not controlled by PHB (Dello Ioio *et al.*, 2012), did not change in ZIC2 treated root meristems or explants (Fig. S8a,b).

Fig. 6 ZIC2 inhibits polar auxin transport. (a) Root growth phenotypes of 6-d-old wild-type seedlings grown on $\frac{1}{2}$ MS medium containing solvent only (CON) or the indicated concentrations of ZIC2. (b) Effect of ZIC2 on root gravitropic response. Five-day-old wild-type seedlings were transferred on vertical half-strength MS agar plates containing the indicated concentrations of either ZIC2 or naphthylphthalamic acid (NPA) and then cultured for further 19 h. After rotating plates by an angle of 90° against vertical direction plants were further incubated for 8 h. Root angles were measured, grouped into 22.5° classes and plotted as circular histograms. (c) Quantification of primary root growth of 5-d-old wild-type seedlings transferred on vertical plates with $\frac{1}{2}$ MS medium CON or the indicated concentrations of NPA or ZIC2. Increase in root length was measured 48 h after transfer (means \pm SEM; $n \geq 20$). Different letters over the error bars indicate significant differences ($P < 0.05$; one-way ANOVA followed by Tukey's multiple comparison tests). (d) Quantification of primary root length of wild-type seedlings germinated for 4 d on $\frac{1}{2}$ MS medium and then transferred on vertical plates with $\frac{1}{2}$ MS medium CON or the indicated concentrations of NPA or ZIC2. Root length was measured 4 d after transfer (means \pm SEM; $n \geq 8$). Different letters over the error bars indicate significant differences ($P < 0.05$; one-way ANOVA followed by Tukey's multiple comparison tests). (e) Quantification of lateral root primordia of wild-type seedlings germinated for 4 d on $\frac{1}{2}$ MS medium and then transferred on vertical plates with half-strength MS medium CON or the indicated concentrations of NPA or ZIC2. Root primordia were counted 4 d after transfer (means \pm SEM; $n \geq 8$). Different letters over the error bars indicate significant differences ($P < 0.05$; one-way ANOVA followed by Tukey's multiple comparison tests). (f) Quantification of lateral root primordia of wild-type seedlings germinated for 4 d on $\frac{1}{2}$ MS medium and then transferred on vertical plates with half-strength MS medium CON or the indicated concentrations of NPA or ZIC2. Root primordia were counted 8 d after transfer (means \pm SEM; $n \geq 8$). Different letters over the error bars indicate significant differences ($P < 0.05$; one-way ANOVA followed by Tukey's multiple comparison tests). (g) Lugol-staining of 7-d-old wild-type primary root tips treated with the indicated concentrations of NPA and ZIC2. Plants were germinated for 4 d on $\frac{1}{2}$ MS medium and then transferred to drug-containing $\frac{1}{2}$ MS medium for 3 d. (h) Effect of NPA and ZIC2 on DR5::GUS activity (upper panel) pARR5::GUS activity (middle panel) and pPIN1::GUS activity (lower panel) in root tips of wild-type seedlings. Plants were germinated for 4 d on $\frac{1}{2}$ MS medium and then transferred on $\frac{1}{2}$ MS medium CON, 25 μ M NPA or 25 μ M ZIC2. GUS staining was performed 4 d after transfer. (i) Transport of carbon-14 (14 C)-labelled indole-3-acetic acid (IAA) in 2.5-cm wild-type inflorescence stem pieces. Data from at least three biological repeats are shown (means \pm SEM). Data were analysed using one-way ANOVA followed by Tukey's multiple comparison tests. Significant differences ($P < 0.05$) are indicated by different letters in each segment group. Bars: (a) 0.5 mm; (g, h) 100 μ m.



ZIC2 inhibits polar auxin transport

Seedlings grown on ZIC2-containing medium showed a defect in root gravitropism. This defect was already clearly apparent at a concentration of 1 μM and was fully developed at a

concentration of 5 μM (Fig. 6a). ZIC2 inhibited root gravitropism in a concentration range comparable with the polar auxin transport inhibitor NPA (Fig. 6b). Block of polar auxin transport by NPA also suppresses primary root growth as well as the formation of lateral root primordia (Rashotte *et al.*, 2000; Casimiro

et al., 2001). Both processes are also affected by ZIC2 (Fig. 6c–f). ZIC2 application also caused the formation of additional starch granule-containing columella cell layers (Fig. 6g), a hallmark of NPA-treated root meristems (Sabatini *et al.*, 1999). These anatomical changes triggered by the two drugs were accompanied by highly congruent alterations in DR5::GUS, ARR5::GUS and pPIN1::GUS expression patterns of root tips (Figs 6h, S9a). Moreover, ZIC2 led to enhanced DR5::GUS activity in the margins of cotyledons (Fig. S9b), another feature provoked by auxin transport inhibitor treatment (Bao *et al.*, 2004). Finally, we compared the movement of radioactively labelled auxin through inflorescence stems pretreated with either NPA or ZIC2. Both compounds blocked accumulation of the [14 C]-IAA in the basal segments of treated stems (Fig. 6i). However, in contrast to NPA (Abas *et al.*, 2021), ZIC2 did not significantly alter PIN1/3 auxin transport activities in *Xenopus* oocytes (Fig. S10a,b). Taken together, ZIC2 provokes NPA-like growth defects and inhibits polar auxin transport *in planta*, but does not directly affect PIN auxin transport in a heterologous test system.

Block of auxin transport by NPA causes accumulation of HD-ZIP III transcripts and enhances shoot regeneration in *Arabidopsis*

To test, whether the promotive effect of ZIC2 on HD-ZIP III expression and shoot regeneration is due to its impact on polar auxin transport, we analyzed the effect of NPA on these processes. Increasing concentrations of NPA caused strengthening and broadening of the pZPR3::GUS expression pattern in the root tip as observed for ZIC2 (Fig. 7a). Accordingly, NPA and ZIC2 exhibited the same inductive effect on gPHB::GUS activity resulting in strong reporter expression in the proliferating stele tissues of the RAM (Fig. 7b). Moreover, addition of NPA to the shoot induction medium led to a significantly higher shoot cluster number in a concentration range between 1 and 25 μ M (Fig. 7c,d). The higher regeneration rate was accompanied by stronger and broader ZPR3 and PHB expression domains, which subsequently co-localized with the higher number of regenerating shoots (Fig. 7e,f).

Altered auxin responses in ZIC2-treated explants correlate with the suppression of root development and a subsequent higher rate of shoot formation

To better understand how ZIC2-mediated inhibition of auxin transport leads to the enhanced shoot regeneration rate we monitored auxin responses during the regeneration process. In the first 5 d on SIM, DR5rev::GFP activity was prevalent in the proliferating pericycle cells and the reporter activity appeared slightly stronger after treatment with the drug (Fig. S11a). Thereafter, DR5 reporter expression marked root primordium formation in the control sample, which did not occur in the presence of ZIC2 (Fig. S11a,b). The inability to form functional root primordia on ZIC2 was also reflected in altered PIN1 expression patterns. pPIN1::GUS activity was present in deformed non-growing protuberances (Fig. S11c). These structures showed unorganized

pPIN1::PIN:GFP localization in contrast to the root primordia in the control samples (Fig. S11d). However, 12 d after transfer, new PIN1 and DR5 expression domains appeared at a higher density on the surface of ZIC2-treated explants compared to the control samples, representing incipient shoot meristems (Fig. S11b,c,e). Taken together, auxin transport inhibition by ZIC2 interferes with root primordia formation and promotes HD-ZIP III expression, which activates a developmental program favorable for shoot regeneration.

ZIC2 and NPA promote *de novo* shoot formation in the regeneration recalcitrant species sunflower

To assess, whether ZIC2 improves *de novo* shoot formation in regeneration recalcitrant plant species, we tested the compound in sunflower using cotyledons as explants (Sujatha *et al.*, 2012). ZIC2 caused a significant increase in the size of forming shoot meristem clusters (Fig. 8a–d). This correlated with a higher level of *HaWUS* expression in ZIC2-treated explants (Fig. 8i). The higher density of regenerated meristems also resulted in a higher number of outgrowing shoots when transferred on gibberellin-containing shoot elongation medium (Fig. 8j). Moreover, ZIC2 application also raised the percentage of shoot regenerating explants (Fig. 8e). A dose response experiment revealed 10 μ M as the most favorable concentration in respect to SAM cluster size as well as regeneration frequency (Fig. 8g,h). We also tested the structural analogs of ZIC2 in sunflower and consistent with the results in *Arabidopsis* (Fig. S4), only T6 exerted a promotive effect in the recalcitrant crop (Fig. 8f).

Finally, NPA also considerably enhanced *de novo* shoot formation, when applied in our sunflower regeneration protocol, in a comparable concentration range as ZIC2 (Fig. 8k–m). Thus, pharmacological modulation of auxin transport can be used to improve shoot regeneration rates in the recalcitrant species sunflower.

Discussion

De novo shoot regeneration enables plants to continue organogenesis even after massive damage of their body structures. Moreover, it constitutes the foundation of biotechnical methods central for basic plant research and crop breeding. In this work we identified ZIC2 as a novel small molecule modulator of polar auxin transport to induce the expression of HD-ZIP III proteins and thereby to promote the rate of shoot regeneration in *Arabidopsis*. Our results provide insight that local HD-ZIP III induction in explant tissue, is controlled by auxin gradients formed by polar transport of the hormone. We moreover show that this knowledge can be applied to enhance *in vitro* shoot formation in the regeneration-recalcitrant crop sunflower.

ZIC2 inhibits polar auxin transport *in planta* and provokes morphological and molecular phenotypes closely related to the auxin efflux inhibitor NPA. NPA directly targets PIN auxin efflux carriers and interferes with their activity by affecting their dimerization behavior (Abas *et al.*, 2021; Teale *et al.*, 2021).

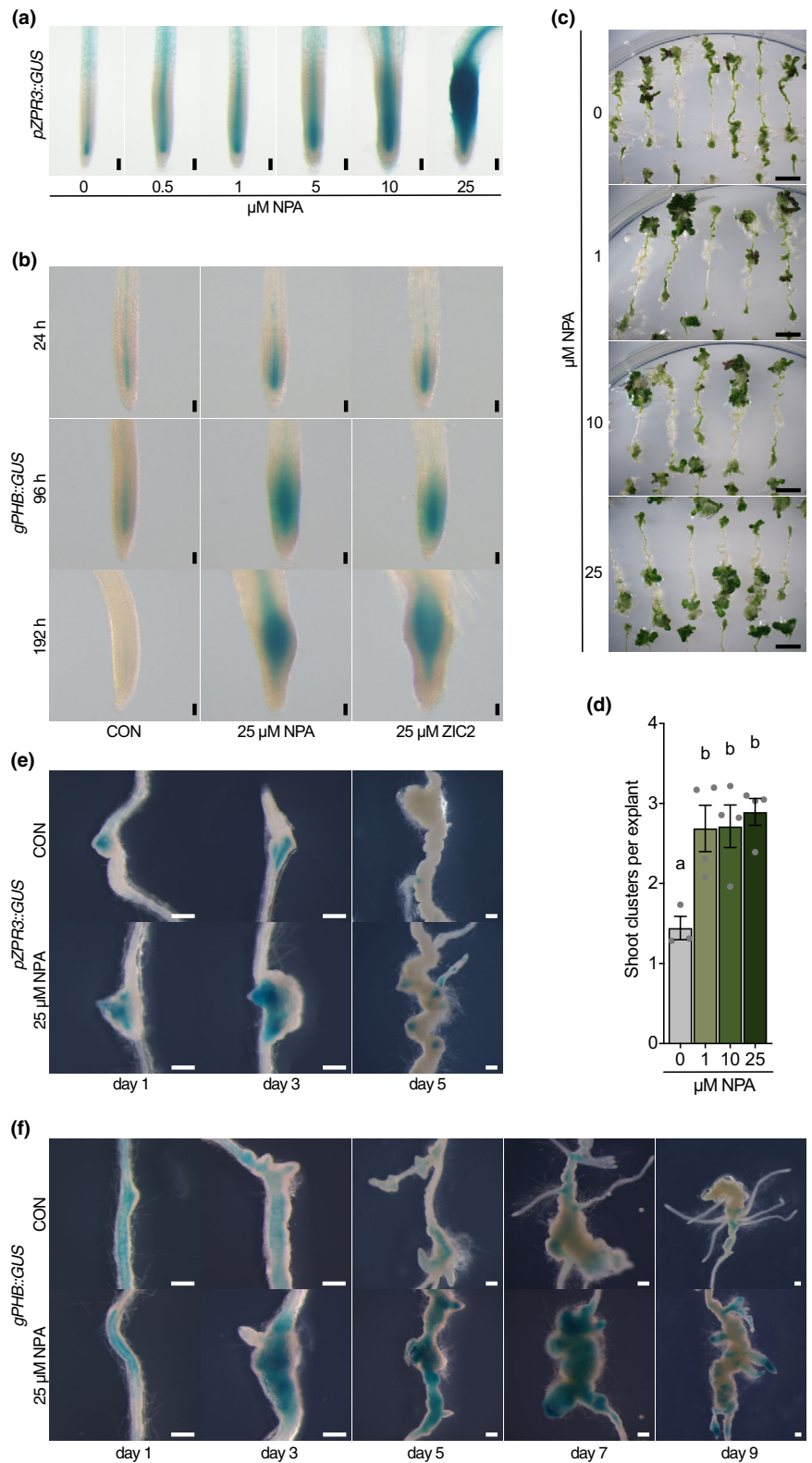
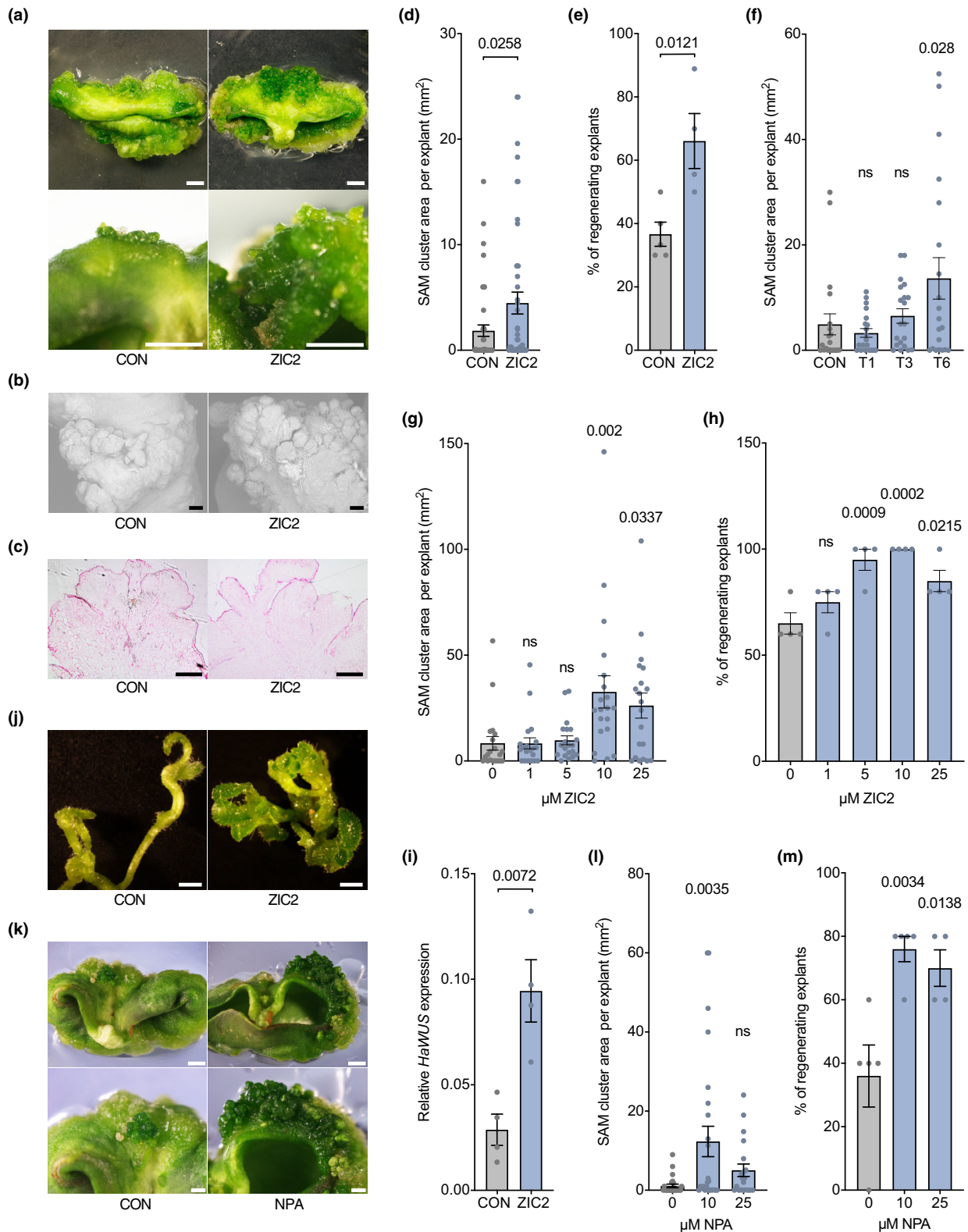


Fig. 7 Block of auxin transport by naphthylphthalamic acid (NPA) causes accumulation of Class III homeodomain-leucine zipper transcripts and enhances shoot regeneration in *Arabidopsis*. (a) pZPR3::GUS activity in primary roots of wild-type seedlings 8 d after germination (DAG) grown on the indicated concentrations of NPA. (b) gPHB::GUS expression in primary roots of wild-type plants grown for the indicated times on medium containing only the solvent dimethyl sulfoxide (DMSO) (CON), 25 μM NPA or 25 μM ZIC2. Plants were germinated on $\frac{1}{2}$ MS medium and transferred on compound-containing media at 4 DAG. (c) Shoot regeneration phenotypes of wild-type explants cultivated on shoot induction medium (SIM) containing the indicated concentrations of NPA. Photographs were taken 16 d after transfer on SIM. (d) Quantification of shoot regeneration rate (shoot clusters per explant) in wild-type explants cultivated on SIM containing the indicated concentrations of NPA. Bars show means \pm SEM from at least three independent experiments ($n \geq 12$ for each experiment). Different letters over the error bars indicate significant differences ($P < 0.05$; one-way ANOVA followed by Tukey's multiple comparison tests). (e) pZPR3::GUS activity in explants cultured on SIM containing solvent only (CON) or 25 μM NPA for the indicated number of days. (f) gPHB::GUS activity in explants cultured on SIM CON or 25 μM NPA for the indicated number of days. Bars: (a, b) 100 μm ; (c) 5 mm; (e, f) 200 μm .

However, in contrast to NPA, ZIC2 does not impede the activity of heterologous expressed PIN proteins suggesting that ZIC2 impacts on auxin transport by a different molecular mechanism. This finding is consistent with the low structural similarity of ZIC2 to NPA and other members of the phytotropin family of

auxin transport inhibitors (Katekar *et al.*, 1981). ZIC2 neither shows structural resemblance to other classical auxin transport inhibitors such as 2,3,5-triiodobenzoic acid (TIBA) or morphactin nor to more recently identified compounds we found in the literature (Rojas-Pierce *et al.*, 2007; Kim *et al.*, 2010; Tsuda



et al., 2011; Nishimura *et al.*, 2012; Steenackers *et al.*, 2017). We therefore postulate that ZIC2 represents a novel type of polar auxin transport inhibitor. Future studies should clarify whether ZIC2 specifically acts on other known NPA targets involved in auxin transport such as the ABCB family of multidrug efflux

proteins (Noh *et al.*, 2001) or affects yet unknown regulators of this process.

Local induction of HD-ZIP III expression in explants has been shown to be a prerequisite for the establishment of shoot stem cell niches (T. Q. Zhang *et al.*, 2017). However, how this domain

Fig. 8 ZIC2 enhances shoot regeneration in sunflower. (a) Shoot regeneration phenotypes of sunflower cotyledon explants cultivated on regeneration medium containing solvent only (CON) or 25 μ M ZIC2. Photographs were taken 21 d after transfer on regeneration medium. Overview pictures are shown in upper panel, close up views of regenerating areas are shown in lower panel. (b) Scanning electron micrographs of regenerating areas of sunflower cotyledon explants cultivated on regeneration medium CON or 25 μ M ZIC2 for 21 d. (c) Transversal sections of regenerating areas of sunflower cotyledon explants cultivated on regeneration medium CON or 25 μ M ZIC2 for 35 d. (d) Quantification of shoot apical meristem (SAM) cluster area of sunflower cotyledon explants cultivated on regeneration medium CON or 25 μ M ZIC2 for 21 d (means \pm SEM, $n \geq 45$). *P*-value is indicated above bars (unpaired Student's two-tailed *t*-test). (e) Percentage of regenerating sunflower cotyledon explants on regeneration medium CON or 25 μ M ZIC2. Data from at least four independent repeats are shown (means \pm SEM). *P*-value is indicated above bars (unpaired Student's two-tailed *t*-test). (f) Quantification of SAM cluster area of sunflower cotyledon explants cultivated on regeneration medium CON or 25 μ M of the ZIC2 analogs T1, T3 or T6 (means \pm SEM, $n \geq 20$). Relevant *P*-values obtained from significance test against the control treatment are indicated above bars (ns, not significant; one-way ANOVA followed by Dunnett's multiple comparison test). (g) Quantification of SAM cluster area of sunflower cotyledon explants cultivated on regeneration medium containing the indicated concentrations of ZIC2 for 21 d (means \pm SEM, $n \geq 20$). Relevant *P*-values obtained from significance test against the control treatment are indicated above bars (ns, not significant; one-way ANOVA followed by Dunnett's multiple comparison test). (h) Percentage of regenerating sunflower cotyledon explants on regeneration medium containing the indicated concentrations of ZIC2 for 21 d. Data from four independent repeats are shown (means \pm SEM). Relevant *P*-values obtained from significance test against the control treatment are indicated above bars (ns, not significant; one-way ANOVA followed by Dunnett's multiple comparison test). (i) Quantitative polymerase chain reaction (qPCR) expression analysis of *HaWUS* in sunflower cotyledon explants cultivated for 21 d on shoot regeneration medium CON or 25 μ M ZIC2. Data from four biological repeats are shown (means \pm SEM). *P*-value is indicated above bars (unpaired Student's two-tailed *t*-test). (j) Regenerated shoots from sunflower cotyledon explants cultivated on regeneration medium CON or 25 μ M ZIC2 for 21 d and then transferred on shoot elongation medium for 45 d. (k) Shoot regeneration phenotypes of sunflower cotyledon explants cultivated on regeneration medium CON or 25 μ M naphthylphthalamic acid (NPA). Photographs were taken 21 d after transfer on regeneration medium. Overview pictures are shown in upper panel, close up views of regenerating areas are shown in lower panel. (l) Quantification of SAM cluster area of sunflower cotyledon explants cultivated on regeneration medium containing the indicated concentrations of NPA for 21 d (means \pm SEM, $n \geq 20$). Relevant *P*-values obtained from significance test against the control treatment are indicated above bars (ns, not significant; one-way ANOVA followed by Dunnett's multiple comparison test). (m) Percentage of regenerating sunflower cotyledon explants on regeneration medium containing the indicated concentrations of NPA for 21 d. Data from four independent repeats are shown (means \pm SEM). Relevant *P*-values obtained from significance test against the control treatment are indicated above bars (one-way ANOVA followed by Dunnett's multiple comparison test). Bars: (a, j) 2 mm; (b, c) 250 μ m.

specific induction of HD-ZIP III expression is achieved was not resolved so far. Our analysis of ZIC2 function revealed that the formation of auxin gradients by auxin efflux carriers plays an important role in the transcriptional activation of PHB and its paralogs in explants on SIM. ZIC2-mediated altered distribution of auxin in the explant might directly enhance HD-ZIP III transcription in broader domains, resulting in a higher number of independent shoot stem cell niches formed. Previous studies have provided evidence that auxin controls HD-ZIP III expression. In the SAM, the expression of REV is upregulated by simultaneous application of NPA and the synthetic auxin NAA (Caggiano *et al.*, 2017). During the formation of the primary vascular system and the vascular cambium auxin maxima define the expression domains of HD-ZIP III members (Donner *et al.*, 2009; Ursache *et al.*, 2014; Smetana *et al.*, 2019). In contrast, during the establishment of the shoot stem cell niche in the embryo and the leaf axil, HD-ZIP III expression is rather specified in domains of low auxin response (Shi *et al.*, 2016; Z. Zhang *et al.*, 2017). Although we monitored changes in the expression pattern of auxin responsive DR5::GUS/GFP reporters in ZIC2-treated explants, we could not clearly link the onset and location of ectopic HD-ZIP III expression to areas of enhanced or reduced auxin responsiveness in these tissues. Future time-lapse co-expression experiments of HD-ZIP III reporters with different auxin response detection systems might help to further resolve this issue.

The original aim of the performed small molecule screen was to identify chemicals, which modulate HD-ZIP III activity by direct binding to one of the putative ligand binding domains present in the protein. Our work, however, revealed that ZIC2 promotes HD-ZIP III transcription by compromising auxin transport rather than post-translationally controlling the activity

of these proteins. In previous work it has been shown that HD-ZIP III expression and activity is under tight control at different regulatory levels including miRNA165/166, AGO10 and ZPR proteins (Ramachandran *et al.*, 2017). Due to this tight control, overexpression of HD-ZIP III WT versions does not lead to severe phenotypes like root-shoot conversion or leaf adaxialization phenotypes (Magnani & Barton, 2011). Consistent with this, we do not observe such phenotypes in seedlings treated with ZIC2. Nevertheless, in the process of *de novo* shoot regeneration the transcriptional stimulation by ZIC2 in explants is followed by enhanced and ectopic accumulation of PHB, and this upregulation appears to be sufficient to trigger ectopic shoot stem cell niche formation. The disclosed impact of auxin distribution on HD-ZIP III expression during shoot regeneration will help to further resolve the transcriptional regulation of this important class of transcription factors.

The ZIC2-mediated activation of HD-ZIP III expression is accompanied by an induction of their downstream targets WUS and RAP2.6L, crucial drivers of shoot regeneration (Che *et al.*, 2006; T. Q. Zhang *et al.*, 2017; Yang *et al.*, 2018). In addition, we observed a concerted transcriptional activation of members of the IPT family of cytokinin biosynthesis enzymes resulting in stronger cytokinin responses in regenerating explants. This activation is in agreement with the observation that in the root meristem PHB induces the transcription of IPT1 and IPT7 (Dello Ioio *et al.*, 2012). Thus, in the context of *de novo* shoot regeneration, this downstream effect of HD-ZIP III activity might reinforce the establishment of shoot stemness by enhancing tissue-specific cytokinin responses including B-type ARR activity. Based on these findings, we postulate that during shoot regeneration HD-ZIP III contributes to WUS activation in a dual manner, by binding to its promoter and by enhancing the

activity of their transcriptional interaction partners, the B-type ARRs.

Due to their impact on plant growth and development it is not surprising that PAT inhibitors have been previously tested in organ regeneration experiments in plant tissue culture but the spectrum of observed effects was quite controversial. Consistent with our results, studies in different species revealed a promotive effect of PAT inhibitors on shoot regeneration. In *Arabidopsis* cotyledons, NPA treatment increased the capacity of shoot formation under high light conditions (Nameth *et al.*, 2013) and application of TIBA significantly promoted *de novo* shoot regeneration from cucumber cotyledon explants (Shukla *et al.*, 2014). A positive effect of NPA was also reported for the regeneration of shoots from epicotyl cuttings in different citrus cultivars (Hu *et al.*, 2017). Other studies, however, revealed a clear negative impact of TIBA or NPA on the process of *de novo* shoot regeneration (Murashige, 1965; Cheng *et al.*, 2013). These contradictory results potentially originate from the differences in used explant types, application time points and inhibitor concentrations and this might also be the reason that PAT inhibitors are yet not commonly perceived as regeneration promotive agents. The type of response most likely depends on the levels and distribution of endogenous IAA in the explant and the presence of externally applied auxin in the medium. Moreover, the timepoint and concentration of PAT inhibitor treatment might be crucial to trigger the establishment of the stem cell niche in the early phase of regeneration but to not interfere with the process of leaf formation at later stages. Optimization of application parameters and systemic comparison of different PAT inhibitors with different uptake kinetics and tissue half-lives will reveal to which extent these chemicals can help to overcome regeneration recalcitrance in crop plants and thus a major bottle neck in modern plant breeding.





Acknowledgements

This work was supported by a grant from the German Federal Ministry of Education and Research (BMBF 031B0554 to TS) and grants from the German Research Foundation DFG (SI 2323/2-1 to TS and HA3468/6-3 to UZH). The authors thank Ykä Helariutta and Michael Prigge for providing seed material. The authors also thank Jesica Fabro for contributing to the set-up of the chemical screen as part of her Master thesis. The authors thank Irene Ziegler and Shuyao Chen for technical assistance. Light microscopy was performed at the Center for Advanced Light Microscopy (CALM) at the TUM School of Life Sciences.

Author contributions

TS conceived the study. SY, MdH, JM, DPJ, UZH and TS performed experiments. SY, MdH, JM, UZH, BP and TS evaluated the data and SY and TS performed the statistical analyses. TS drafted the manuscript, which was reviewed and edited by all coauthors.

ORCID

Ulrich Z. Hammes  <https://orcid.org/0000-0002-3663-4908>
 Brigitte Poppenberger  <https://orcid.org/0000-0003-1020-0500>
 Tobias Sieberer  <https://orcid.org/0000-0002-4462-9260>
 Saiqi Yang  <https://orcid.org/0000-0002-6425-3731>

Data availability

All data associated with this manuscript will be made available upon request.

References

- Abas L, Kolb M, Stadlmann J, Janacek DP, Lukic K, Schwecheimer C, Sazanov LA, Mach L, Friml J, Hammes UZ. 2021. Naphthylphthalamic acid associates with and inhibits PIN auxin transporters. *Proceedings of the National Academy of Sciences, USA* 118: e2020857118.
- Altpeter F, Springer NM, Bartley LE, Blechl A, Brutnell TP, Citovsky V, Conrad L, Gelvin SB, Jackson D, Kausch AP *et al.* 2016. Advancing crop transformation in the era of genome editing. *Plant Cell* 28: 1510–1520.
- Bao F, Shen J, Brady SR, Muday GK, Asami T, Yang Z. 2004. Brassinosteroids interact with auxin to promote lateral root development in *Arabidopsis*. *Plant Physiology* 134: 1624–1631.
- Benkova E, Michniewicz M, Sauer M, Teichmann T, Seifertova D, Jurgens G, Friml J. 2003. Local, efflux-dependent auxin gradients as a common module for plant organ formation. *Cell* 115: 591–602.
- Caggiano MP, Yu X, Bhatia N, Larsson A, Ram H, Ohno CK, Sappl P, Meyerowitz EM, Jonsson H, Heisler MG. 2017. Cell type boundaries organize plant development. *eLife* 6: e27421.
- Carlsbecker A, Lee J-Y, Roberts CJ, Dettmer J, Lehesranta S, Zhou J, Lindgren O, Moreno-Risueno MA, Vátén A, Thitamadee S *et al.* 2010. Cell signalling by microRNA165/6 directs gene dose-dependent root cell fate. *Nature* 465: 316–321.
- Casimiro I, Marchant A, Bhalerao RP, Beekman T, Dhooge S, Swarup R, Graham N, Inzé D, Sandberg G, Casero PJ *et al.* 2001. Auxin transport promotes *Arabidopsis* lateral root initiation. *Plant Cell* 13: 843–852.
- Che P, Lall S, Nettleton D, Howell SH. 2006. Gene expression programs during shoot, root, and callus development in *Arabidopsis* tissue culture. *Plant Physiology* 141: 620–637.
- Cheng ZJ, Wang L, Sun W, Zhang Y, Zhou C, Su YH, Li W, Sun TT, Zhao XY, Li XG *et al.* 2013. Pattern of auxin and cytokinin responses for shoot meristem induction results from the regulation of cytokinin biosynthesis by AUXIN RESPONSE FACTOR3. *Plant Physiology* 161: 240–251.
- D'Agostino IB, Deruere J, Kieber JJ. 2000. Characterization of the response of the *Arabidopsis* response regulator gene family to cytokinin. *Plant Physiology* 124: 1706–1717.
- De Smet I, Chaerle P, Vanneste S, De Rycke R, Inze D, Beekman T. 2004. An easy and versatile embedding method for transverse sections. *Journal of Microscopy* 213: 76–80.
- Dello Ioio R, Galinha C, Fletcher A, Grigg S, Molnar A, Willemsen V, Scheres B, Sabatini S, Baulcombe D, Maini P *et al.* 2012. A PHABULOSA/cytokinin feedback loop controls root growth in *Arabidopsis*. *Current Biology* 22: 1699–1704.
- Diener AC, Li H, Zhou W, Whoriskey WJ, Nes WD, Fink GR. 2000. Sterol methyltransferase 1 controls the level of cholesterol in plants. *Plant Cell* 12: 853–870.
- Donner TJ, Sherr I, Scarpella E. 2009. Regulation of preprocambial cell state acquisition by auxin signaling in *Arabidopsis* leaves. *Development* 136: 3235–3246.
- Fastner A, Absmanner B, Hammes UZ. 2017. Use of *Xenopus laevis* oocytes to study auxin transport. *Methods in Molecular Biology* 1497: 259–270.

- Friml J, Vieten A, Sauer M, Weijers D, Schwarz H, Hamann T, Offringa R, Jurgens G. 2003. Efflux-dependent auxin gradients establish the apical-basal axis of *Arabidopsis*. *Nature* 426: 147–153.
- Gillmor CS, Park MY, Smith MR, Pepitone R, Kerstetter RA, Poethig RS. 2010. The MED12-MED13 module of Mediator regulates the timing of embryo patterning in *Arabidopsis*. *Development* 137: 113–122.
- Grigg SP, Galinha C, Kornet N, Canales C, Scheres B, Tsiantis M. 2009. Repression of apical homeobox genes is required for embryonic root development in *Arabidopsis*. *Current Biology* 19: 1485–1490.
- Gross-Hardt R, Lenhard M, Laux T. 2002. WUSCHEL signaling functions in interregional communication during *Arabidopsis* ovule development. *Genes & Development* 16: 1129–1138.
- He J, Xu M, Willmann MR, McCormick K, Hu T, Yang L, Starker CG, Voytas DF, Meyers BC, Poethig RS. 2018. Threshold-dependent repression of SPL gene expression by miR156/miR157 controls vegetative phase change in *Arabidopsis thaliana*. *PLoS Genetics* 14: e1007337.
- Hellens RP, Edwards EA, Leyland NR, Bean S, Mullineaux PM. 2000. pGreen: a versatile and flexible binary Ti vector for *Agrobacterium*-mediated plant transformation. *Plant Molecular Biology* 42: 819–832.
- Hu W, Fagundez S, Katin-Grazzini L, Li Y, Li W, Chen Y, Wang X, Deng Z, Xie S, McAvoy RJ *et al.* 2017. Endogenous auxin and its manipulation influence in vitro shoot organogenesis of citrus epicotyl explants. *Horticulture Research* 4: 17071.
- Ikeuchi M, Favero DS, Sakamoto Y, Iwase A, Coleman D, Rymen B, Sugimoto K. 2019. Molecular mechanisms of plant regeneration. *Annual Review of Plant Biology* 61: 377–406.
- Ikeuchi M, Sugimoto K, Iwase A. 2013. Plant callus: mechanisms of induction and repression. *Plant Cell* 25: 3159–3173.
- Katekar GF, Nave JF, Geissler AE. 1981. Phytotropins: III. NAPHTHYLPHTHALAMIC ACID BINDING SITES ON MAIZE COLEOPTILE MEMBRANES AS POSSIBLE RECEPTOR SITES FOR PHYTOTROPIN ACTION. *Plant Physiology* 68: 1460–1464.
- Kim JY, Henrichs S, Bailly A, Vincenzetti V, Sovero V, Mancuso S, Pollmann S, Kim D, Geisler M, Nam HG. 2010. Identification of an ABCB/P-glycoprotein-specific inhibitor of auxin transport by chemical genomics. *Journal of Biological Chemistry* 285: 23309–23317.
- Kim YS, Kim SG, Lee M, Lee I, Park HY, Seo PJ, Jung JH, Kwon EJ, Suh SW, Paek KH *et al.* 2008. HD-ZIP III activity is modulated by competitive inhibitors via a feedback loop in *Arabidopsis* shoot apical meristem development. *Plant Cell* 20: 920–933.
- Liu Q, Yao X, Pi L, Wang H, Cui X, Huang H. 2009. The *ARGONAUTE10* gene modulates shoot apical meristem maintenance and establishment of leaf polarity by repressing miR165/166 in *Arabidopsis*. *The Plant Journal* 58: 27–40.
- Magnani E, Barton MK. 2011. A per-ARNT-sim-like sensor domain uniquely regulates the activity of the homeodomain leucine zipper transcription factor REVOLUTA in *Arabidopsis*. *Plant Cell* 23: 567–582.
- Mallory AC, Reinhart BJ, Jones-Rhoades MW, Tang G, Zamore PD, Barton MK, Bartel DP. 2004. MicroRNA control of *PHABULOSA* in leaf development: importance of pairing to the microRNA 5' region. *EMBO Journal* 23: 3356–3364.
- Mayer KF, Schoof H, Haecker A, Lenhard M, Jurgens G, Laux T. 1998. Role of *WUSCHEL* in regulating stem cell fate in the *Arabidopsis* shoot meristem. *Cell* 95: 805–815.
- McConnell JR, Emery J, Eshed Y, Bao N, Bowman J, Barton MK. 2001. Role of *PHABULOSA* and *PHAVOLUTA* in determining radial patterning in shoots. *Nature* 411: 709–713.
- Meng WJ, Cheng ZJ, Sang YL, Zhang MM, Rong XF, Wang ZW, Tang YY, Zhang XS. 2017. Type-B ARABIDOPSIS RESPONSE REGULATORS specify the shoot stem cell niche by dual regulation of *WUSCHEL*. *Plant Cell* 29: 1357–1372.
- Miyashima S, Honda M, Hashimoto K, Tatematsu K, Hashimoto T, Sato-Nara K, Okada K, Nakajima K. 2013. A comprehensive expression analysis of the *Arabidopsis* *MICRORNA165/6* gene family during embryogenesis reveals a conserved role in meristem specification and a non-cell-autonomous function. *Plant and Cell Physiology* 54: 375–384.
- Miyawaki K, Matsumoto-Kitano M, Kakimoto T. 2004. Expression of cytokinin biosynthetic isopentenyltransferase genes in *Arabidopsis*: tissue specificity and regulation by auxin, cytokinin, and nitrate. *The Plant Journal* 37: 128–138.
- Moglich A, Ayers RA, Moffat K. 2009. Structure and signaling mechanism of Per-ARNT-Sim domains. *Structure* 17: 1282–1294.
- Mukherjee K, Burglin TR. 2006. MEKHLA, a novel domain with similarity to PAS domains, is fused to plant homeodomain-leucine zipper III proteins. *Plant Physiology* 140: 1142–1150.
- Muller B, Sheen J. 2008. Cytokinin and auxin interaction in root stem-cell specification during early embryogenesis. *Nature* 453: 1094–1097.
- Murashige T. 1965. Effects of stem-elongation retardants and gibberellin on callus growth and organ formation in tobacco tissue culture. *Physiologia Plantarum* 18: 665–673.
- Nameth B, Dinka SJ, Chatfield SP, Morris A, English J, Lewis D, Oro R, Raizada MN. 2013. The shoot regeneration capacity of excised *Arabidopsis* cotyledons is established during the initial hours after injury and is modulated by a complex genetic network of light signalling. *Plant, Cell & Environment* 36: 68–86.
- Nishimura T, Matano N, Morishima T, Kakinuma C, Hayashi K-I, Komano T, Kubo M, Hasebe M, Kasahara H, Kamiya Y *et al.* 2012. Identification of IAA transport inhibitors including compounds affecting cellular PIN trafficking by two chemical screening approaches using maize coleoptile systems. *Plant and Cell Physiology* 53: 1671–1682.
- Noh B, Murphy AS, Spalding EP. 2001. Multidrug resistance-like genes of *Arabidopsis* required for auxin transport and auxin-mediated development. *Plant Cell* 13: 2441–2454.
- Prigge MJ, Otsuga D, Alonso JM, Ecker JR, Drews GN, Clark SE. 2005. Class III homeodomain-leucine zipper gene family members have overlapping, antagonistic, and distinct roles in *Arabidopsis* development. *Plant Cell* 17: 61–76.
- Radhakrishnan D, Kareem A, Durgaprasad K, Sreeraj E, Sugimoto K, Prasad K. 2018. Shoot regeneration: a journey from acquisition of competence to completion. *Current Opinion in Plant Biology* 41: 23–31.
- Radonic LM, Lewi DM, Lopez NE, Hopp HE, Escandon AS, Bilbao ML. 2015. Sunflower (*Helianthus annuus* L.). *Methods in Molecular Biology* 1224: 47–55.
- Ramachandran P, Carlsbecker A, Etchells JP. 2017. Class III HD-ZIPs govern vascular cell fate: an HD view on patterning and differentiation. *Journal of Experimental Botany* 68: 55–69.
- Rashotte AM, Brady SR, Reed RC, Ante SJ, Muday GK. 2000. Basipetal auxin transport is required for gravitropism in roots of *Arabidopsis*. *Plant Physiology* 122: 481–490.
- Reinhart BJ, Liu T, Newell NR, Magnani E, Huang T, Kerstetter R, Michaels S, Barton MK. 2013. Establishing a framework for the Ad/abaxial regulatory network of *Arabidopsis*: ascertaining targets of class III homeodomain leucine zipper and KANADI regulation. *Plant Cell* 25: 3228–3249.
- Rojas-Pierce M, Titapiwatanakun B, Sohn EJ, Fang F, Larive CK, Blakeslee J, Cheng Y, Cuttler S, Peer WA, Murphy AS *et al.* 2007. *Arabidopsis* P-glycoprotein19 participates in the inhibition of gravitropism by gravacin. *Chemistry & Biology* 14: 1366–1376.
- Rozhon W, Mayerhofer J, Petutschnig E, Fujioka S, Jonak C. 2010. ASKtheta, a group-III *Arabidopsis* GSK3, functions in the brassinosteroid signalling pathway. *The Plant Journal* 62: 215–223.
- Sabatini S, Beis D, Wolkenfelt H, Murfett J, Guilfoyle T, Malamy J, Benfey P, Leyser O, Bechtold N, Weisbeek P *et al.* 1999. An auxin-dependent distal organizer of pattern and polarity in the *Arabidopsis* root. *Cell* 99: 463–472.
- Schrick K, Bruno M, Khosla A, Cox PN, Marlatt SA, Roque RA, Nguyen HC, He C, Snyder MP, Singh D *et al.* 2014. Shared functions of plant and mammalian StAR-related lipid transfer (START) domains in modulating transcription factor activity. *BMC Biology* 12: 70.
- Shi B, Zhang C, Tian C, Wang J, Wang Q, Xu T, Xu Y, Ohno C, Sablowski R, Heisler MG *et al.* 2016. Two-step regulation of a meristematic cell population acting in shoot branching in *Arabidopsis*. *PLoS Genetics* 12: e1006168.
- Shukla PS, Das AK, Jha B, Agarwal PK. 2014. High-frequency in vitro shoot regeneration in *Cucumis sativus* by inhibition of endogenous auxin. *In Vitro Cellular & Developmental Biology-Plant* 50: 729–737.
- Smetana O, Mäkilä R, Lyu M, Amirousofi A, Sánchez Rodríguez F, Wu M-F, Solé-Gil A, Leal Gavarrón M, Siligato R, Miyashima S *et al.* 2019. High levels

- of auxin signalling define the stem-cell organizer of the vascular cambium. *Nature* 565: 485–489.
- Smith ZR, Long JA. 2010. Control of *Arabidopsis* apical-basal embryo polarity by antagonistic transcription factors. *Nature* 464: 423–426.
- Steenackers W, Klíma P, Quareshy M, Cesarino I, Kumpf RP, Corneille S, Araújo P, Viaene T, Goeminne G, Nowack MK *et al.* 2017. cis-Cinnamic acid is a novel, natural auxin efflux inhibitor that promotes lateral root formation. *Plant Physiology* 173: 552–565.
- Sugimoto K, Temman H, Kadokura S, Matsunaga S. 2019. To regenerate or not to regenerate: factors that drive plant regeneration. *Current Opinion in Plant Biology* 47: 138–150.
- Sujatha M, Vijay S, Vasavi S, Reddy PV, Rao SC. 2012. Agrobacterium-mediated transformation of cotyledons of mature seeds of multiple genotypes of sunflower (*Helianthus annuus* L.). *Plant Cell Tissue and Organ Culture* 110: 275–287.
- Takei K, Ueda N, Aoki K, Kuromori T, Hirayama T, Shinozaki K, Yamaya T, Sakakibara H. 2004. AtIPT3 is a key determinant of nitrate-dependent cytokinin biosynthesis in *Arabidopsis*. *Plant and Cell Physiology* 45: 1053–1062.
- Teale WD, Pasternak T, Dal Bosco C, Dovzhenko A, Kratzat K, Bildl W, Schwörer M, Falk T, Ruperti B, V Schaefer J *et al.* 2021. Flavonol-mediated stabilization of PIN efflux complexes regulates polar auxin transport. *EMBO Journal* 40: e104416.
- Tsuda E, Yang H, Nishimura T, Uehara Y, Sakai T, Furutani M, Koshihara T, Hirose M, Nozaki H, Murphy AS *et al.* 2011. Alkoxy-auxins are selective inhibitors of auxin transport mediated by PIN, ABCB, and AUX1 transporters. *Journal of Biological Chemistry* 286: 2354–2364.
- Ulmasov T, Murfett J, Hagen G, Guilfoyle TJ. 1997. Aux/IAA proteins repress expression of reporter genes containing natural and highly active synthetic auxin response elements. *Plant Cell* 9: 1963–1971.
- Ursache R, Miyashima S, Chen Q, Vaten A, Nakajima K, Carlsbecker A, Zhao Y, Helariutta Y, Dettmer J. 2014. Tryptophan-dependent auxin biosynthesis is required for HD-ZIP III-mediated xylem patterning. *Development* 141: 1250–1259.
- Weits DA, Kunkowska AB, Kamps NCW, Portz KMS, Packbier NK, Nemec Venzla Z, Gaillochet C, Lohmann JU, Pedersen O, van Dongen JT *et al.* 2019. An apical hypoxic niche sets the pace of shoot meristem activity. *Nature* 569: 714–717.
- Wenkel S, Emery J, Hou BH, Evans MM, Barton MK. 2007. A feedback regulatory module formed by *LITTLE ZIPPER* and *HD-ZIP III* genes. *Plant Cell* 19: 3379–3390.
- Xiao Y, Offringa R. 2020. PDK1 regulates auxin transport and *Arabidopsis* vascular development through AGC1 kinase PAX. *Nature Plants* 6: 544–555.
- Yang S, Poretska O, Sieberer T. 2018. ALTERED MERISTEM PROGRAM1 restricts shoot meristem proliferation and regeneration by limiting HD-ZIP III-mediated expression of RAP2.6L. *Plant Physiology* 177: 1580–1594.
- Yoo SD, Cho YH, Sheen J. 2007. *Arabidopsis* mesophyll protoplasts: a versatile cell system for transient gene expression analysis. *Nature Protocols* 2: 1565–1572.
- Zhang TQ, Lian H, Zhou CM, Xu L, Jiao Y, Wang JW. 2017. A two-step model for de novo activation of *WUSCHEL* during plant shoot regeneration. *Plant Cell* 29: 1073–1087.
- Zhang ZF, Finer JJ. 2015. Sunflower (*Helianthus annuus* L.) organogenesis from primary leaves of young seedlings preconditioned by cytokinin. *Plant Cell Tissue and Organ Culture* 123: 645–655.
- Zhang Z, Tucker E, Hermann M, Laux T. 2017. A molecular framework for the embryonic initiation of shoot meristem stem cells. *Developmental Cell* 40: 264–277 e264.
- Zhu H, Hu F, Wang R, Zhou X, Sze SH, Liou LW, Barefoot A, Dickman M, Zhang X. 2011. *Arabidopsis* Argonaute10 specifically sequesters miR166/165 to regulate shoot apical meristem development. *Cell* 145: 242–256.

Supporting Information

Additional Supporting Information may be found online in the Supporting Information section at the end of the article.

Fig. S1 Effect of ZIC2 concentration and application time on the induction of pZPR3::GUS activity.

Fig. S2 ZIC2 structure/function analysis.

Fig. S3 ZIC2 does not show direct cytokinin or auxin activity.

Fig. S4 Effect of ZIC2 analogs on *Arabidopsis* shoot regeneration.

Fig. S5 Effect of ZIC2 on post-transcriptional class III homeodomain-leucine zipper activity.

Fig. S6 Effect of ZIC2 on pMIR165A::GFP and pMIR166A::GFP fluorescence in primary root meristems.

Fig. S7 ZIC2 induces the expression of a subset of cytokinin biosynthesis enzymes during *Arabidopsis* shoot regeneration.

Fig. S8 Effect of ZIC2 on pIPT5::GUS activity in primary root meristems and during shoot regeneration.

Fig. S9 Naphtylphtalamic acid-like effects of ZIC2 on auxin responses in *Arabidopsis* seedlings.

Fig. S10 Effect of ZIC2 on PIN-mediated ³H-IAA efflux in *Xenopus* oocytes.

Fig. S11 Effect of ZIC2 and naphtylphtalamic acid on auxin responses during regeneration.

Table S1 Oligos used in quantitative real-time polymerase chain reaction experiments.

Please note: Wiley Blackwell are not responsible for the content or functionality of any Supporting Information supplied by the authors. Any queries (other than missing material) should be directed to the *New Phytologist* Central Office.